Concordia
UNIVERSITY

TN-EMC-94-01
March 31, 1994
Final Report

COMPUTATIONAL STUDIES FOR PREDICTION OF ENERGY DEPOSITION IN HUMANS EXPOSED TO RF FIELDS FROM CELLULAR PHONES

Dr. S.J. Kubina
Dr. C.W. Trueman

FACULTY OF ENGINEERING AND COMPUTER SCIENCE

EMC LABORATORY
RTMENT OF ELECTRICAL AND COMPUTER ENGINEERING
7141 Sherbrooke St. West, L-AD-532
Montreal, Quebec, Canada H4B 1R6

Releasable
CRC-CR-94-009

TN-EMC-94-01
March 31, 1994
Final Report

COMPUTATIONAL STUDIES FOR PREDICTION OF ENERGY DEPOSITION IN HUMANS EXPOSED TO RF FIELDS FROM CELLULAR PHONES

Dr. S.J. Kubina
Dr. C.W. Trueman

Prepared For:

Ministry of Industry, Science and Technology
Communications Research Centre
DSS 36001-3-3603
MIST/CRC 36001-3-3603

Table of Contents

Computational Studies for Prediction of Energy Deposition in Humans Exposed to RF Fields from Cellular Phones

Page

Computational Studies for the Prediction of Energy Deposition in Humans Exposed to RF Fields from Cellular Phones

FINAL REPORT

1.0 INTRODUCTION

This report is intended to summarize the work that was done in an initial research contract for the study of the methodology which could be applied to the computation of the RF fields associated with the use of cellular telephones. The objectives of the research contract are described in the contractual Statement of Work (SOW) that is enclosed as Appendix A.

Important at the start, was a systematic survey of the state-of-the-art in computational modelling of the transceiver and operator plus an identification of the corresponding measurements which would serve to validate the modelling techniques or which would provide additional quantitative information on the energy deposition or external field distribution aspects.

Vital to any further research, is the acquisition or development of a suitable computer model of the transceiver and the human operator. While probing the availability of existing models, the organization and initiation of the development of a finely-stepped (1 mm), discretized model of the human head was launched. At the same time, we began to plan a series of systematic measurements which could eventually be carried out in Canada at the David Florida Laboratory (DFL) of the Canadian Space Agency (CSA).

The Table of Contents of this report reflects our intentions about its scope. This specific presentation was preempted by the request to participate in a Bio-Session at the ANTEM '94 conference in Ottawa on August 2-5, 1994, and chaired by Dr. Maria Stuchly. This offered us an opportunity to summarize our work preparatory for the technical community at large. Since the contents of the paper duplicate the specific portions of this Final Report, it would have been a wasteful duplication of effort at a time of limited resources to reproduce its contents in a different format. Hence, the published paper is reproduced as Appendix B.

However, to keep the outline of the Table of Contents, the body of this report maintains the individual topic sections and provides brief comments which refer to the appendix material. The oral presentation of the paper included some additional material. Thus hardcopies of the illustrations used for the delivery of the paper are also included as Appendix C. Readers will be able to glean the full scope of what was done by scanning the report in this way.

1.1 Survey of Computational Electromagnetic Modelling Methods

A workable survey of computational modelling methods can be found in the several new books on Computational Electromagnetics. They can be categorized as time-domain or frequency domain methods or distinguished by their integral equation or differential equation formulations. Important to this application is the ability to faithfully represent constituent lossy dielectric materials of the operator as well as the conductive radiating structure of the handset. As can be noted in the Statement of Work, our intention is to concentrate on the methods with which we have developed some prior experience, such as the Finite Difference Time-Domain Method and the Moment Method.

1.1.1 The Finite-Difference Time-Domain Method

A compact description is presented in the ANTEM '94 paper to be found in Appendix B. More detailed descriptions are provided in its references.

1.1.2 Finite-Element Methods

See current survey text descriptions.

1.1.3 Moment Methods

Our use of moment methods is best described in the recent work on complex RCS models [1] where comparisons of FDTD results and those with the Numerical Electromagnetics Code are featured.

1.1.4 The Multiple-Multipole Method

See current survey text descriptions.

1.2 Applications to Biological Interactions

The applications to biological interactions are reviewed in the ANTEM '94 paper and its references.

1.2.1 Antenna Performance in the Presence of an Operator

The antenna performance in the presence of an operator is currently best outlined (at cellular phone frequencies) in the work of Anderson et al. shown in Appendix C.

1.2.2 Exposure to RF Fields

The summary comments of the ANTEM '94 paper apply.

1.2.3 Hyperthermia

The summary comments of the ANTEM '94 paper apply as well as the energy deposition curves shown in the oral paper presentation material of Appendix C.

1.3 Electrical Properties Biological Materials

The table of the ANTEM '94 paper apply as well as the dispersion curves of the oral presentation to be found in Appendix C.

1.4 Measurements and Validation

The work of Anderson et al. described in the oral presentation material of Appendix C is representative of available measurements at cellular phone frequencies.

2.0 THE FINITE-DIFFERENCE TIME-DOMAIN METHOD

The summary of the ANTEM '94 paper applies. Its references provide an outline of the necessary adaptations which are required to provide the representation of the transceiver and its radiating antenna and eventually, the dispersive properties of the dielectric materials.

2.1 The FDTD Algorithm

The summary of the ANTEM '94 paper applies.

2.2 FDTD and Radiating Antennas

The summary of the ANTEM '94 paper applies and especially its reference number 7.

2.3 FDTD with Dispersive Materials

The summary of the ANTEM '94 paper plus its references apply as does the additional material of the oral presentation.

3.0 PROGRESS TO DATE AND WORK IN PROGRESS

The material below will indicate the progress made thus far in the development of the discretized head model. In addition, several planning discussions have been held with DFL and CRC on the extent and timing of a measurement sequence ranging from handset alone, with phantoms, and eventually with a human operator.

3.1 Modelling of the Cellular Phone

Specifications and form factors of available handsets have been sought. Any initial representations of the external field of the handset alone will likely use NEC wire-grid models which can be used for initial measurement checkout and then for comparisons with subsequent FDTD modelling.

3.2 Code Acquisition and Modification

Recent technical conferences have been used to discuss the availability of FDTD and Moment Method codes which have already been adapted to this problem. No firm commitments have been obtained, since each investigator seems to have the codes in a fluid state.

3.3 Head Phantoms

The material of the oral presentation in Appendix C indicates the type of head phantoms that are available.

The colour illustrations of the head models shown in Appendix C also indicate the model development progress which has been made. It is important to derive these models to launch the computations, either to trade or compare with others and to have a complete and thorough understanding of their composition.

It is also important to remember that eventually discretized models of the phantoms will be required in order to match the corresponding measurement results.

4.0 ACKNOWLEDGEMENTS

The collaboration of Dr. Wilfred Lauber and his patient direction are gratefully acknowledged. Dr. Maria Stuchly was an invaluable source of information and guide on work that is now being done at other laboratories. Discussions with Dr. Shantnu Mishra of DFL have been giving us the encouragement that meaningful measurements can soon be incorporated into this project.

The dedicated and meticulous work of our research assistant, Mina Danesh, gave us an encouraging start with the head model development.

5.0 REFERENCES

[1] Trueman, C.W. and Kubina, S.J., "HF Ground Wave Radar Studies," Final Report, TN-EMC-94-02, DSS/DREO Contract No. W7714-3-9707/01-SV, EMC Laboratory, Electrical & Computer Engineering, Concordia University, August 1994.

6.0 APPENDICES

Appendix A - Statement of Work, Computational Studies for Prediction of Energy Deposition in Humans Exposed to RF Fields from Cellular Phones, Contract Number MIST/CRC 36001-3-3603

Appendix B - Paper Presented at the ANTEM '94 Conference, Ottawa, August 2-5, 1994

Appendix C - Illustrations Used for Oral Presentation of Paper, ANTEM '94 Conference, Ottawa, August 2-5, 1994

APPENDIX A

Statement of Work, Computational Studies for Prediction of Energy Deposition in Humans Exposed to RF Fields from Cellular Phones
Contract Number MIST/CRC 36001-3-3603

30 August 1993

Statement of Work

Computational Studies for Prediction of Energy Deposition in Humans Exposed to RF Fields from Cellular Phones

Aims and Objectives

The aim of this project is to study the most promising methods of computational modelling which can be applied to predict the energy deposition levels in the human head exposed to the RF fields of modern hand-held cellular telephones. A validated computational methodology would form an essential part of the research aimed at assessing the RF safety of these devices.

This study will concentrate on the frequency band (~900 MHz) presently in use and will serve as a base of evaluation of the methodology for its extension to the higher planned frequencies for personal communications.

Technical Approach

The exploratory work on this project shall be directed at the survey of the state-of-art of the modelling and measurements in this field, the acquisition of all the physical parameters associated with human body composition and the RF cellular devices, the analysis of the external field distribution (and correlation with known reliable measurement data), in preparation for the volumetric modelling of sources and human body (head, shoulders, arms..) by an adaptation of the FDTD computer programs that are currently in use at the EMC Laboratory.

1. State-of-Art Review

All available literature sources will be examined, with the assistance of DOC, to establish the extent of available modelling information on this problem at frequencies in the cellular radio bands (initially focusing at 900 MHz), corresponding measurement data and the relevant physical parameters of the sources and irradiated subject.

2. Definition of Physical Parameters

From the literature survey, data at the Department of Health and Welfare and any subsequent measurements or estimates, the e.m. properties of the human subject will be catalogued in relation to an appropriate geometric description to be used in the computational modelling at the frequencies specified for this initial study.

Particular note shall be taken of the frequency dispersion of these parameters.

The physical and RF properties of the sources (cellular devices and test dipoles) shall be catalogued for use in the source modelling aspect of the external and internal problem with the most likely computer codes.

3. Analysis of the External Problem

One or two of the available EFIE, or Hybrid integral equation-based codes shall be used to model the external field distribution produced by the sources used in measurements. This is necessary for the realistic definition of source fields to be used with the FDTD method. Comparisons with modelling data of other investigators will be made at this stage.

Close collaboration and contact will be maintained with DOC and the measurement program which is planned to take place as a part of this program.

4. Volumetric Modelling - FDTD

The volumetric modelling of the upper portions of the subject and sources will be carried out in a methodical manner starting with exploratory testing of crude models to simulate published results to the progressive refinement of the discretization of the subject and source to simulate actual measurements that will be undertaken with a phantom and later, human subjects.

Testing will be done with select Gaussian excitations in the available FDTD formulations to concentrate on the applicable frequency bands and also to gain some experience with the frequency dispersion aspects of the modelling problem.

Reporting Requirements

Brief Summary Quarterly Reports will be prepared to coincide with the invoicing periods as usually required under contract. Yearly Summary Status Reports will be provided and a formal Final Report will be provided.

As work progresses, conference and journal papers will be prepared and cleared with the Technical Authority.

Dr. S. J. Kubina, Eng.
30th August 1993

APPENDIX B

Paper Presented at the ANTEM '94 Conference
Ottawa, Ontario
August 2-5, 1994

CELLULAR PHONES AND HUMANS- A NEOPHYTE OUTLOOK

S.J. Kubina
C.W. Trueman
EMC Laboratory
Concordia University
Montreal, Quebec

W. Lauber
Communications
Research Centre
Ottawa, Ontario

S.R. Mishra
David Florida Laboratory
Canadian Space Agency
Ottawa, Ontario

Abstract-A cellular phone is a portable radio that radiates 0.6 watt from an antenna located very close to the operator's head. Concern has been expressed as to whether a cellular phone is capable of inducing damaging field strengths inside the user's head. This paper reviews the application of electromagnetic modelling techniques using the finite-difference time-domain(FDTD) method to this problem. The construction of an FDTD model of the cellular phone and of the head is discussed. The relative permittivity and conductivity of biological tissue varies with frequency, and this paper reviews modifications of the FDTD method to handle such dispersive media. Some specific applications of measurement methods and of the FDTD method to the calculation of the amount of electromagnetic power delivered to the body are discussed.

Introduction

Recently concern has been expressed by the general public and the news media over whether cellular telephones pose a health risk[1]. Cellular phones operate between 824 and 850 MHz, and radiate 0.6 watt of power. Cellular phone sets meet the existing standard for portable radio sets[2], which limit the power that the radio can cause the body to absorb. Tissue damage largely depends on heating due to power delivered by the electromagnetic field[1], given by the "specific absorption rate"(SAR) in watts per kilogram. Standards limit the power absorption to 80 mW/kg average SAR over the entire body, and 1.6 W/kg peak SAR to any 1 gram of tissue for 30 minutes or more. If a device radiates less than 0.74 W at the frequency of cellular phones, it is considered absolutely safe because it cannot deliver the limiting power levels outlined above.

This paper discusses computational modelling of the head in three dimensions, for the purpose of determining the local SAR levels throughout its volume when a cellular phone is in use. The emphasis is on the "finite-difference time-domain"(FDTD) method, although a variety of other techniques are also feasible[3,4]. We will review the basics of FDTD and how an FDTD model of a cellular phone and a head is constructed. Techniques for modelling the dispersive nature of biological tissue will be discussed, and then we will touch on some results that have been published that are pertinent to the assessment of cellular phone hazards.

The Finite-Difference Time-Domain Method

In Yee's finite-difference time-domain method[5], space is subdivided into cells of size Δx by Δy by Δz and time into steps of size Δt. The partial derivatives in Maxwell's curl equations are replaced by central-difference formulas involving the components of the electric field along the edges of the cells, and the components of the magnetic field normal to the faces of the cells. Initially all the fields are zero. The time function for the generator voltage is known and is used to obtain a known electric field applied at the base of the antenna. Time is advanced in steps of Δt, and

at each time step, the value of the electric field component along each edge of each cell is calculated and then the value of the magnetic field component perpendicular to the center of each cell face is found, using Yee's "leap frog" update scheme. The electric field at time step $(n + 1/2)$ is found from its previous value and the adjacent magnetic field values at step n. Then the magnetic field at step $(n + 1)$ is updated from its previous value and from the adjacent electric fields at step $(n + 1/2)$. In this way the generator voltage is used to determine the electric and magnetic fields throughout the cell space as a function of time.

The FDTD cell space size of N_x by N_y by N_z cells is usually limited by computer resources to $N_xN_yN_z$ =500,000 or perhaps 1,000,000 cells, although more might be used if a supercomputer is available. The cell space contains the cellular phone and head models at its center, separated from the outer boundary by a layer of free-space cells. Field components within the cell space are computed with the Yee FDTD algorithm. Field components on the outer surfaces of the cell space are updated using an "absorbing boundary condition"(ABC), which is intended to cause the outer surfaces of the cell space to absorb all the energy incident upon them. The most common ABC is the second-order Mur boundary[6]. Because the ABC is imperfect, there can be a significant amount of reflection from the outer boundary. A sufficiently large number of free-space cells must separate the surfaces of the FDTD model from the outer boundary, such that interactions between the model and the outer boundary are reduced to insignificant levels.

The bandwidth of the FDTD cell model extends up to the frequency where the cell size is one-tenth of the wavelength in the dielectric material that has the shortest wavelength. The largest time step Δt that can be used in FDTD is called the "Courant Limit", and for cubical cells is given by $\Delta t = \Delta x/(\sqrt{3}\,c)$, where Δx is the cell size and c is the free-space speed of light. The speed-of-light in the FDTD grid is somewhat dependent on the direction of travel of the wave; the error is larger as the frequency approaches the grid's limiting frequency.

Modelling a Person Operating a Cellular Phone

To model a cellular phone operating near a person's head, cells at appropriate locations must be given material properties to represent the cellular phone itself, its antenna, and the head. The cellular phone is modelled by specifying a parallelepiped block of cells to be perfectly-conducting, representing the electrical circuit board and internal components[7]. The plastic case can be modelled with a layer of cells set to a typical relative permittivity for plastic, such as $\varepsilon_r \approx 2$[7]. The phone's wire antenna is modelled by setting the electric field to zero along the edges of the cells which lie in a straight line along the path of the wire; currently available techniques require the antenna to be parallel to the x –, or y –, or z –axis. Special care is taken in updating the magnetic field components at the centers of the cell faces adjacent to the antenna[8]. The antenna is excited by specifying the voltage time function applied to the base of the antenna, which is used to specify the electric field on the cell edge modelling the base of the antenna[7] at each time step.

From the electromagnetic point of view, a head is made up of regions of lossy dielectric with various permittivities and conductivities. To build an FDTD model of the head, each cell in the model is assigned electrical parameters appropriate to the tissue at the cell's location: skin, bone, eye, muscle, brain, and so forth. The FDTD update equations for the components of the electric field in each cell use the permittivity and conductivity for that cell. In updating electric field components that lie on the boundaries between cells having differing material types, a weighted average of

the permittivity and conductivity of each cell should be used[9,10]. This is included as a volume-averaged permittivity in Ref. [11], accounting for the fraction of a cell occupied by free-space compared to that composed of, for example, muscle.

Antenna Source Voltage Functions

The source voltage is applied as an electric field across the gap at the base of the antenna. The source time function must not contain any frequency components above the bandwidth for the FDTD cell space. If the source voltage time function is to be a sine wave, then it must turn on gradually, as an abrupt start would violate the grid's bandwidth restriction. Then the FDTD algorithm must be run for a sufficient number of time steps that the turn-on transients die away, and sinusoidal steady-state to be reached. For high-permittivity resonant structures, a great many time steps may be required[9], as very long time constants are involved. Under certain circumstances, resonance is encountered in electromagnetic models of human beings[12]. When steady-state is reached each field component in the grid will be sinusoidal, and the amplitude and phase can be determined from the time history for the last period of the input function.

To obtain the frequency response over a wide bandwidth, the FDTD code is often run with a sine wave input many times at individual frequencies. Alternately, we can take advantage of FDTD's solution of Maxwell's Equations in the time domain to obtain information over a wide bandwidth in a single run. The source voltage can be a Gaussian pulse or other time-limited function whose spectral content is restricted to bandwidth for which the FDTD grid is valid. Then the FDTD algorithm finds the time response of each field component in the cell space due to the source voltage pulse. Again, the FDTD algorithm must be run for a sufficient number of time steps to trace the transient response of each field component to zero value. The Fourier transform is used to find the response as a function of frequency. Yee's FDTD assumes that neither the conductivity nor the permittivity vary with frequency, and must be modified to model biological tissues over wide bandwidths, as discussed below.

Computing the Radiated Fields

The FDTD method obtains the time functions giving the value of the electric fields on each of the cell edges, and the corresponding magnetic fields at the centers of the cell faces, at each time step. These near field time functions are used to find the far fields or radiated fields of the cellular phone operating near the head, with a near-zone to far-zone transformation[13]. Thus at each time step, the far field in any direction can be found from the values of the near fields on a closed integration surface, usually taken to be a few cells inside the absorbing boundary of the cell space.

Electrical Parameters of Biological Materials

To construct an electromagnetic model of a human being, detailed anatomical information is required. Ref. [14] gives cross-sections of the head and body at approximately 2.5 cm spacing, obtained by dissection. By superimposing the grid of FDTD cells on each cross-section, it is possible to assign a tissue type to each cell. Ref. [15] constructed a cell model of a person in this way, assigning one of 14 different material types to each cell. For computation the cell size was 1.31 cm, with a total of about 145,000 cells in the model. At each frequency the relative permittivity of each of the tissue types are found from the literature[3,16-21] and are listed in Tables 1 and 2 for tissues relevant to modelling the head. Note that the permittivity of some types of tissue is quite high, and that both permittivity and conductivity change very significantly in the frequency range covered by the tables.

Table 1
The permittivity of biological materials at various frequencies.

Tissue	Ref	Frequency (MHz) 10	27.12	100	350	400	500	750	900	1000	1500
Brain,	3	163-352		57-90						37-55	
nerve	3		155	52	60						
	16							49			46
	17			63		50.3			41.2		
	20				74						
Bone,	3	37		23							
Fat	3		29	7.5	5.7						
	16							5.6			5.6
	17			12.2		9.2			7.3		
	20				5.7						
Muscle	3	162-204		64-90						57-59	
	3		106	74	53						
	16							52			49
	17			70.5		62.5			54.7		
	18			71-76			52-54			49-52	
	19			63		52.6	52.4		52		
	21								50.5		
	20				54						
Skin	3		106	25	17.6						
	16							52			49
	18			57			46.5			43-46	
	20					17.4					
Eye	3		155	85	80						
	16							80			80
Blood	3		102	74	65						
	18			69-81			67-70			60.5	
	20				65						

Modelling Dispersive Materials with FDTD

Tables 1 and 2 illustrate that tissue is quite "dispersive", that is, the permittivity and conductivity of tissue varies quite rapidly with frequency. But in Yee's FDTD the relative permittivity ε_r and conductivity σ cannot change with frequency. To obtain the fields inside a model of a head or body over a wide frequency band, the FDTD code must be run with a sine wave excitation at many individual frequencies, with the appropriate permittivity and conductivity at each frequency. But we lose the inherent advantage of a time domain method, in which the response to a pulse input function obtains wideband information in a single run. To regain this capability, the FDTD algorithm must be modified to directly incorporate the dispersive nature of biological materials.

Table 2
The conductivity of biological materials at various frequencies.

Tissue	Ref	Frequency (MHz) 10	27.12	100	350	400	500	750	900	1000	1500
Brain,	3	0.21-0.63		0.48-0.95						0.81-1.2	
nerve	3		0.45	0.53	0.65						
	16							1.2			1.4
	17			4.7		7.5			12.2		
	20				0.62						
Bone,	3	0.024		0.057							
Fat	3		0.04	0.07	0.072						
	16							0.09			0.12
	17			0.215		0.88			1.4		
	20				0.07						
Muscle	3	0.69-0.96		0.75-1.05						1.38-1.45	
	3		0.74	1.0	1.33						
	16							1.54			1.77
	17			6.8		9			13.8		
	19			0.62		0.68	0.72		0.92		
	21								1.2		
	20				1.3						
Skin	3		0.74	0.55	0.44						
	16							1.54			1.77
	17				0.42						
Eye	3		0.45	1.9	1.9						
	16							1.9			1.9
Blood	3		0.28	1.1	1.2						
	20				1.22						

The simplest model of materials with frequency-dependent permittivity and conductivity is given by the Debye equation[3]. The frequency dependence of the complex relative permittivity is described with a single relaxation time, according to

$$\varepsilon_r(\omega) = \varepsilon_{r\infty} + \frac{\varepsilon_{rs} - \varepsilon_{r\infty}}{1 + j\omega\tau}$$

where ω is the operating frequency in rad/sec, $\varepsilon_{r\infty}$ is the relative permittivity at high frequencies, ε_{rs} is the "static" relative permittivity at zero frequency, and τ is the relaxation time. Ref. [22] describes a frequency-dependent finite-difference time-domain or $(FD)^2TD$ method. The relation between the electric flux density, the frequency-dependent permittivity and the electric field in the frequency domain

$$D(\omega) = \varepsilon_r(\omega)\varepsilon_0 E(\omega)$$

becomes a convolution in the time domain. Ref. [22] modifies the Yee FDTD algorithm to compute the convolution as a running sum, which must be maintained for each location in the cell space. Water, which has a slowly-varying permittivity in the range 0 to 80 GHz, is modelled with $\varepsilon_{rs} = 81$, $\varepsilon_{r\infty} = 1.8$, and relaxation time $\tau = 9.4$ picoseconds with good agreement with the exact solution in a one-dimensional geometry.

Ref. [23] applies the $(FD)^2TD$ method to model muscle from 40 to 433 MHz. The relative permittivity of muscle varies with frequency much more rapidly than that of water. At 40.68 MHz, it is 97.3, declining to 53 at 433 MHz, while the conductivity rises from 0.693 S/m at 40.68 MHz to 1.43 at 433 MHz[24]. Ref. [23] choses $\varepsilon_{r\infty} = 15$, $\varepsilon_{rs} = 120$, $\sigma = 0.64$ S/m and relaxation time $\tau = 6.67$ nanoseconds to obtain a reasonable representation of the frequency dependence of the relative permittivity and conductivity of muscle from 40 to 400 MHz. The paper models a two-dimensional cylindrical structure with $(FD)^2TD$ and compares the result to the exact solution in the form of a Bessel function series evaluated at individual frequencies, with excellent agreement.

Ref. [25] extends the $(FD)^2TD$ method to handle multiple second-order Lorentz poles. The permittivity is represented as

$$\varepsilon_r = \varepsilon_{r\infty} + (\varepsilon_{rs} - \varepsilon_{r\infty}) \sum_{p=1}^{P} \frac{G_p \omega_p^2}{\omega_p^2 + 2j\omega\delta_p - \omega^2}$$

where $\sum_{p=1}^{P} G_p = 1$, P is the number of poles, and ω_p and δ_p are the resonant frequency and damping coefficient, respectively, of the p-th pole. The method is an extension of the convolution technique used in Ref. [22] for a simple Debye pole. Ref. [26] extends the method to include multiple simple poles of the Debye type as well as complex poles.

Ref. [11] offers an alternate formulation for $(FD)^2TD$ based on the solution of a differential equation relationship between the electric flux density D and the electric field E at each time step. The method is applied to model material properties in terms of two simple Debye poles, that is, using two relaxation times. Ref. [27] gives the permittivity of muscle in terms of five relaxation times, valid over a wide frequency range. In Ref. [26] the representation is simplified to use only two time constants, to obtain a reasonable representation of frequency variation of muscle's permittivity from 20 MHz to 20 GHz. The $(FD)^2TD$ method is applied to the parts of a whole-body model composed of muscle to calculate induced currents in the body at 40, 150 and 350 MHz.

Ref. [28] provides estimates of the parameters required to represent 12 types of biological tissue with the two relaxation time model, valid up to 3 GHz. Each tissue has its individual values of the two "static" permittivities, and the "high frequency" permittivity required for the dispersion model. But all the tissue types are modelled as having the same relaxation times τ_1 and τ_2. This permits the actual permittivity of each cell of the FDTD model to be chosen by volume averaging according to the fraction of the cell occupied by each type of tissue. This improves the resolution of models having a somewhat coarse cell size. Then a single run of the $(FD)^2TD$ code obtains the field strengths in each cell up to 915 MHz, which would require many runs of the Yee FDTD code with a single-frequency sine wave excitation.

SAR Studies using the FDTD Method

It is thought that the principal cause for concern for exposure to electromagnetic fields such as those radiated by cellular phones is due to the heating of tissue. The "specific absorption rate"(SAR) gives the rate at which energy is supplied to tissue, or the power supplied per unit mass, and is given for one cell of an FDTD model by

$$SAR = \frac{\sigma}{2\rho}(E_x^2 + E_y^2 + E_z^2)$$

where σ is the conductivity, E_x, E_y, and E_z are amplitudes of the x, y, and z components of the sinusoidally-varying electric fields, and ρ is the mass density of the tissue in the cell. Most studies seek to evaluate the SAR for comparison with safety standards.

Before computational methods that are able to handle dielectric materials became available, measurements were the only means to determine the radiation patterns of portable radios operated near a human head or body. Indeed measurements will continue to provide a quick and accurate means of determining whether cellular phone antenna provides adequate coverage. A typical measurement uses a "head phantom" filled with a material designed to simulate the average electrical properties of biological tissue[29]. Also, embedded field strength probes or temperature probes in a head phantom may provide a useful means of confirming the accuracy of field strength or SAR values obtained by computation. Ref. [30] used a whole-body phantom to measure the power absorbed by a person near a cellular phone antenna on a car. The car phone system is designed to radiate between 3 and 10 watts. The study showed that, for a child standing 15 cm from the antenna, which is very close, the antenna would have to radiate 35 watts to exceed the safety standard.

Ref. [29] considered the energy deposited in the head by a portable radio at 840 MHz, with a whip antenna and a sleeve dipole. The radio differs from a cellular phone in that it is normally held in front of the face with the antenna extending vertically near the operator's eyes and forehead. In Ref. [20] the temperature rise in a head phantom was measured. A "hot spot" was found near the antenna, but the associated temperature rise was so small that there is no potential for tissue damage.

Ref. [20] studied the energy absorbed by a human in the field of a distant antenna, represented by an incident plane wave. Ref. [20] used an FDTD model of the torso having 1.27 cm cells, derived from the cross-sectional anatomy of Ref. [14]. The material properties of each cell were assigned depending on the volume fraction of the cell occupied by each tissue type. The torso model had 16628 cells, and was centered in a space of 36 by 24 by 44 cells for a total of 38016 cells. A sinusoidal excitation was used at both 100 MHz and 433 MHz, with time stepping for three cycles to reach steady state. The SAR was determined for cross-sections of the torso. The study was extended in Ref. [15]. The torso model was extended to become a complete model of a "standard man" 175 cm tall, weighing 70 kg. At 100 MHz, 2.62 cm cells were used with an FDTD space size of 23x12x68 or 18768 cells. At 350 MHz, 1.31 cm cells were used for better resolution, and the overall space used 45x24x135 or 145800 cells. As before, a sinusoidal source was used, and time-stepping was carried out for three cycles to reach "steady state". It was found that at 100 MHz there is a considerable difference between the SAR in the body isolated in space compared to the body standing on a ground plane, but at 350 MHz, there is not much difference.

Ref. [21] studied the changes in the performance of a handheld telephone set at 900 MHz and 1900 MHz due to the presence of the operator's hand and head. The telephone set was modelled as a perfectly-conducting box with a quarter-wave monopole on top. The hand and the head were represented as pure muscle tissue. The head was modelled as a sphere of radius 9 cm; the hand was a block 10 cm wide and 2 cm thick wrapped around the lower part of the telephone set. The excitation was a Gaussian pulse modulated with a cosine wave, permitting the impedance and other parameters to be found over a small bandwidth around the cosine's frequency. The total number of cells in the model was 141,680; time stepping was carried out for 1500 steps. The input impedance of the antenna and the azimuth radiation pattern of the FDTD model were compared with the measured impedance and pattern of a real person holding the telephone set. The changes in the impedance and azimuth pattern of the telephone set due to the operator that were expected from the FDTD model were found in the measurement. However, the model was too simple to predict these quantities precisely.

FDTD is often used to study the problem of hyperthermia, in which an applicator is applied to the body to deliver electromagnetic energy to a tumor, which is then destroyed by electromagnetic heating. Ref. [31] studied the use of dipoles to apply energy to tumors at 70 and 95 MHz. In this application, CAT scans taken of an individual patient's body were used to construct an FDTD model with 34751 cells. The FDTD model predicts the internal SAR values when energy is applied with a standard array of dipoles, excited with a sinusoid at a single frequency. The objective is to design the excitation of the array to achieve high SAR in the tumor, but low absorption rates elsewhere to prevent damage to healthy tissue.

Ref. [28] used $(FD)^2TD$ to study the SARs in the whole body when exposed to a plane wave. As discussed above, the electrical parameters of each tissue type were described with a dispersion model using two relaxation times, valid to 3 GHz. The method was used to find the SAR averaged over layers of the body at frequencies from 20 to 915 MHz, due to plane wave exposure. $(FD)^2TD$ allows the computation of the fields in the body as a function of time due to a narrow pulse, which contains energy over a wide range of frequencies. Ref. [28] graphs the net current induced at various cross-sections of the body as a function of time, including the dispersive effects of the tissues.

Conclusion

Because of the concerns of the general public that cellular phone operation might have an associated health risk, there is tremendous interest and activity in predicting field strengths and specific absorption rates inside the head. But at present there is little published work dealing specifically with the SAR in the head at the frequency of cellular telephones. Existing studies of hazards associated with radiofrequency fields were used to develop the standard maximum field strengths and power levels[2] such that, to the best of available knowledge, cellular telephones pose no health risk. As discussed in this paper, the analytic and numerical tools for detailed accurate computation of field strength levels inside the head have greatly improved in the past five years. We can expect a landslide of information as these methods are applied to assess the SAR levels to be expected in the head when using a cellular phone.

Acknowledgement

Dr. M.A. Stuchly's assistance in supplying reference material is gratefully acknowledged.

References

1. M. Fischetti, "The Cellular Phone Scare", Special Report/Communications, IEEE Spectrum, pp. 43-47, June, 1993.
2. "IEEE Standard for Safety Levels with Respect to Human Exposure to Radio Frequency Electromagnetic Fields, 3 kHz to 3 GHz", IEEE C95.1-1991, IEEE, Piscataway, New Jersey.
3. O.P. Gandhi, Editor, "Biological Effects and Medical Applications of Electromagnetic Energy", Prentice-Hall, New Jersey, 1993.
4. N. Kuster and Q. Balzano, "Energy Absorption Mechanism by Biological Bodies in the Near Field of Dipole Antennas Above 300 MHz", IEEE Transactions on Vehicular Technologies, Vol. VT-41, No. 1, pp. 17-23, February, 1992.
5. K.S. Yee, "Numerical Solution of Initial Value Problems Involving Maxwell's Equations in Isotropic Media", IEEE Trans. on Antennas and Propagation, Vol. AP-14, No. 3, pp. 302-307, May, 1966.
6. G. Mur, "Absorbing Boundary Condition for the Finite-Difference Approximation of the Time-Domain Electromagnetic Field Equations", IEEE Trans. on Electromagnetic Compatibility, Vol. EMC-23, No. 4, November, 1981.
7. R. Luebbers, L. Chen, T. Uno, and S. Adachi, "FDTD Calculation of Radiation Patterns, Impedance, and Gain for a Monopole Antenna on a Conducting Box", IEEE Transactions on Antennas and Propagation, Vol. 40, No. 12, pp. 1577-1583, December, 1992.
8. K.R. Umashankar, A. Taflove and B. Beker, "Calculation and Experimental Validation of Induced Currents on Coupled Wires in an Arbitrary Shaped Cavity", IEEE Trans. on Antennas and Propagation, Vol. AP-35, No. 11, pp. 1248-1257, November, 1987.
9. C.W. Trueman, R.J. Luebbers, S.R. Mishra and C. Larose, "RCS of High Permittivity Cubes Computed by FDTD with Prony Extrapolation", Third International Conference on Electromagnetics in Aerospace Applications, Torino, Italy, September 14-17, 1993.
10. J.G. Maloney and G.S. Smith, "A Comparison of Methods for Modeling Electrically Thin Dielectric and Conducting Sheets in the Finite-Difference Time-Domain (FDTD) Method", IEEE Trans. on Antennas and Propagation, Vol. 41, May, 1993.
11. O.P. Gandhi, B-Q Gao and J-Y Chen, "A Frequency-Dependent Finite-Difference Time-Domain Formulation for General Dispersive Media", IEEE Trans. on Microwave Theory and Techniques, Vol. MTT-41, No. 4, pp. 658-665, April, 1993.
12. M.J. Hagmann, O.P. Gandhi, J.A. D'Andrea and I. Chatterjee, "Head Resonance: Numerical Solutions and Experimental Results", IEEE Trans. on Microwave Theory and Techniques, Vol. MTT-27, No. 9, pp 809-813, September, 1979.
13. R.J. Luebbers, K.S. Kunz, M. Schneider and F. Hunsberger, "A Finite-Difference Time-Domain Near Zone to Far Zone Transformation", IEEE Trans. on Antennas and Propagation, Vol. AP-39, No. 4, April, 1991.
14. A.C. Eycleshymer and D.M Schoemaker, "A Cross-Section Anatomy", D. Appleton and Co., New York, 1911.
15. D.M. Sullivan, O.P. Gandhi and A. Taflove, "Use of the Finite-Difference Time-Domain Method for Calculating EM Absorption in Man Models", IEEE Trans. on Biomedical Engineering, Vol. BME-35, No. 3, pp. 179-186, March, 1988.
16. A. Taflove and M. E. Brodwin, "Computation of the Electromagnetic Fields and Induced Temperatures within a Model of the Microwave-Irradiated Human Eye", IEEE Transactions on Microwave Theory and Techniques, Vol. MTT-23, No. 11, pp. 888-896, November, 1975.
17. G. Hartsgrove, A. Kraszewski, and A. Surowiec, "Simulated Biological Materials for Electromagnetic Radiation Absorption Studies", Bioelectromagnetics, Vol. 8, pp. 29-36, 1987.

18. M. A. Stuchly and S. S. Stuchly, "Dielectric Properties of Biological Substances - Tabulated", Microwave Power, 15(1), pp. 19-26, 1980.
19. W. T. Joines, Y. Zhang, C. Li, and R. L. Jirtle, "The Measured Electrical Properties of Normal and Malignant Human Tissues From 50 to 900 MHz", Medical Physics, Vol. 21, No. 4, pp. 547-550, April 1994.
20. D. M. Sullivan, D. T. Borup, and O. P. Gandhi, "Use of Finite-Difference Time-Domain Method in Calculating EM Absorption in Human Tissues", IEEE Transactions on Biomedical Engineering, Vol. BME-34, No. 2, pp. 148-157, February, April, 1987.
21. J. Toftgard, S.N. Hornsleth, and J. B. Andersen, "Effects on Portable Antennas of the Presence of a Person", IEEE Trans. on Antennas and Propagation, Vol. AP-41, No. 6, pp. 739-746, June, 1993.
22. R. Luebbers, F. P. Hunsberger, K. S. Kunz, R. B. Standler, and M. Schneider, "A Frequency-Dependent Finite-Difference Time-Domain Formulation for Dispersive Materials", IEEE Transactions on Electromagnetic Compatibility, Vol. 32, No. 3, pp. 222-227, August, 1990.
23. D.M. Sullivan, "A Frequency-Dependent FDTD Method for Biological Applications", IEEE Trans. on Microwave Theory and Techniques, Vol. MTT-40, No. 3, pp. 532-539, March, 1992.
24. C.C. Johnson and A.W. Guy, "Nonionizing Electromagnetic Wave Effects in Biological Materials and Systems", Proc. IEEE, Vol. 60, pp. 692-718, June, 1972.
25. R. Luebbers and F. Hunsberger, "FDTD for N-th Order Dispersive Media", IEEE Trans. on Antennas and Propagation, Vol. AP-40, No. 11, pp. 1297-1301, November, 1992.
26. R. Luebbers, D. Steich and K. Kunz, "FDTD Calculation of Scattering from Frequency-Dependent Materials", IEEE Trans. on Antennas and Propagation, Vol. AP-41, No. 9, pp. 1249-1257, September, 1993.
27. W.P. Hurt, "Multiterm Debye Dispersion Relations for Permittivity of Muscle", IEEE Trans. Biomed. Eng., Vol. BME-32, pp. 60-63, 1985.
28. C.M. Furse, J.-Y. Chen and O.P. Gandhi, "The Use of the Frequency-Dependent Finite-Difference Time-Domain Method for Induced Current and SAR Calculations for a Heterogeneous Model of the Human Body", IEEE Trans. on Electromagnetic Compatibility, Vol. EMC-36, No. 2, pp. 128-133, May, 1994.
29. Q. Balzano, O. Garay, and F. R. Steel, "Heating of Biological Tissue in the Induction Field of VHF Portable Radio Transmitters", IEEE Transactions on Vehicular Technology, Vol. VT-27, No. 2, pp. 51-56, May, 1978.
30. A.W. Guy and C-K Chou, "Specific Absorption Rates of Energy in Man Models Exposed to Cellular UHF Mobile-Antenna Fields", IEEE Trans. on Microwave Theory and Techniques, Vol. MTT-34, No. 6, pp. 671-680, June, 1986.
31. D. Sullivan, "Three Dimensional Computer Simulation in Deep Regional Hyperthermia Using the Finite-Difference Time-Domain Method", IEEE Transactions on Microwave Theory and Techniques, Vol. MTT-38, No. 2, pp. 204-211, February, 1990.

APPENDIX C

Illustrations Used for Oral Presentation of Paper Presented at ANTEM '94 Conference
Ottawa, Ontario
August 2-5, 1994

CELLULAR PHONES AND HUMANS - A NEOPHYTE OUTLOOK

S.J. Kubina*, C. W. Trueman*, W. Lauber** and S. R. Mishra

*Concordia University
** CRC Ottawa
DFL/SPA

Antem 94

Purpose of Paper

- *Our Goal: Internal/External Flds- Modelling/Measurements*
- *Bio-Materials*
- *Models and Phantoms*
- *Modelling*
- *Measurements*
- *Target Methods: Computational/Measurement*

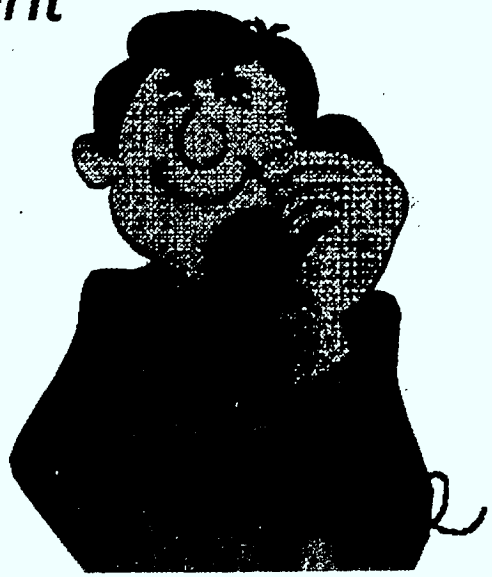

Antem 94

CONSIDERATIONS

- *Physical*
  - *Set - Form Factors*
  - *Humans - m/f/c*
- *Electromagnetic*
  - *Frequency*
  - *Antenna/Feed*
  - *Polarization*
  - *Power*
  - *.....next.....*

Antem 94

3a

Bell Mobility

Cellular Service

Components for cellular handsets, PCN and private radio networks.

l technology
pell huge
nies

:s
ou-
ır

CONSIDERATIONS (Cont'd)

- Electromagnetic ...
  - Radiation Pattern
    - Volumetric
  - Near Field Structure
    - External
  - Internal Fields
    - Deposition Rates

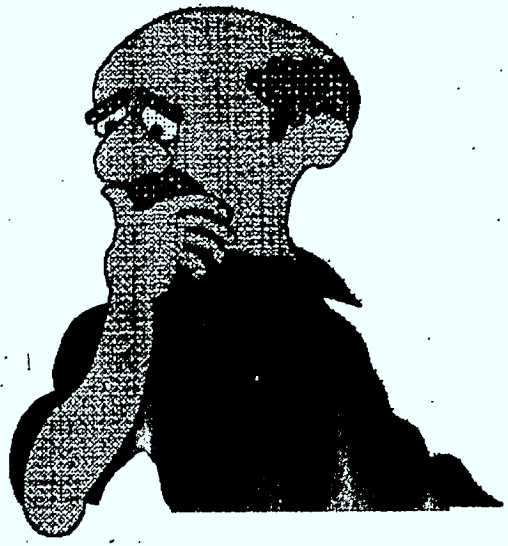

ANATOMICAL MODELS & PHANTOMS

- Primary Source
  - Eycleshymer & Schoemaker 1911
- Utah - Prof. Om Ghandi et al.
- University of Ottawa
- Commercial
- Other...

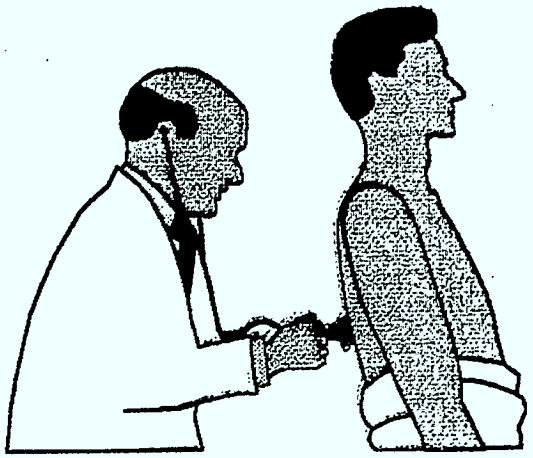

Antem 94

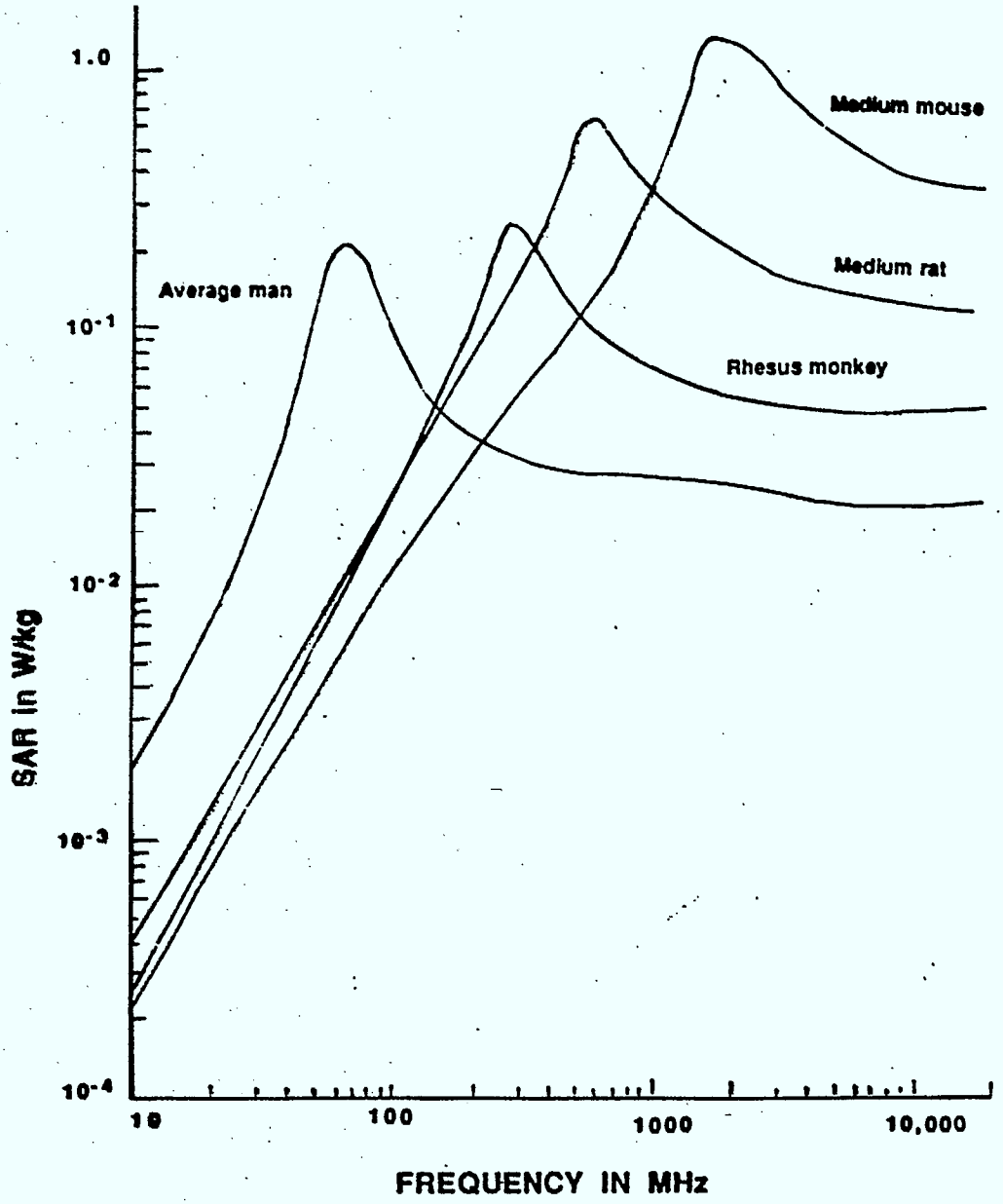

Figure 8-3 Whole-body-averaged specific absorption rate of prolate spheroidal models of average man, rhesus monkey, medium rat, and medium mouse for E polarization at incident plane-wave power density of 1 mW/cm^2. (From Durney, C. H., Johnson, C. C., Barber, P. W., et al. [1978]. Radiofrequency radiation dosimetry handbook, 2nd ed. Pub. No. SAM-TR-78-22, USAF School of Aerospace Medicine (RZP), Aerospace Medical Division (AFSC), Brooks Air Force Base, Tex.)

from Gandhi, Om P., Ed., "Biological Effects and Medical Applications of Electromagnetic Energy," Prentice Hall, 1990, ISBN 0-13-082728-2.

5a
→ 9a)

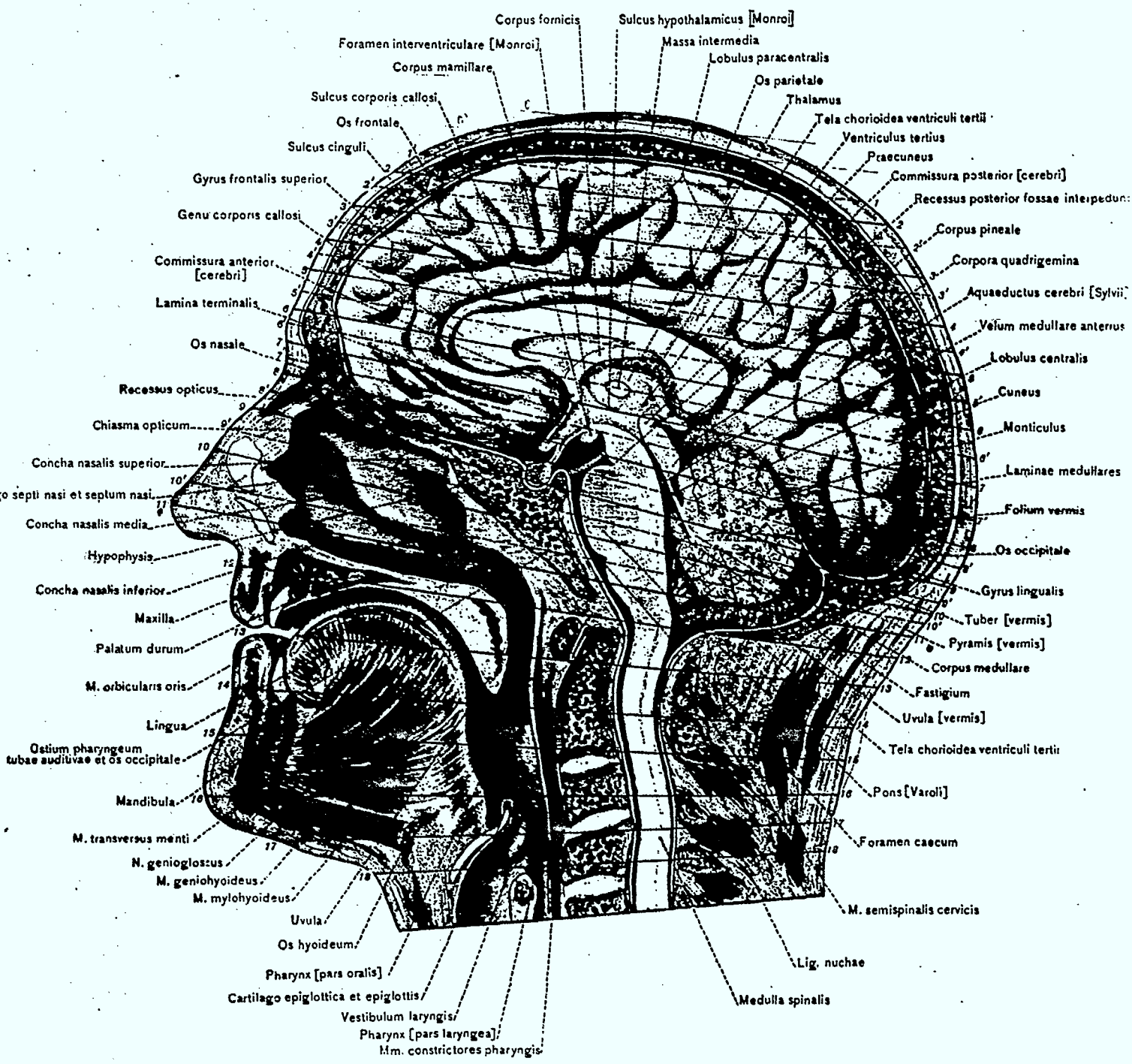

KEY-FIGURE III

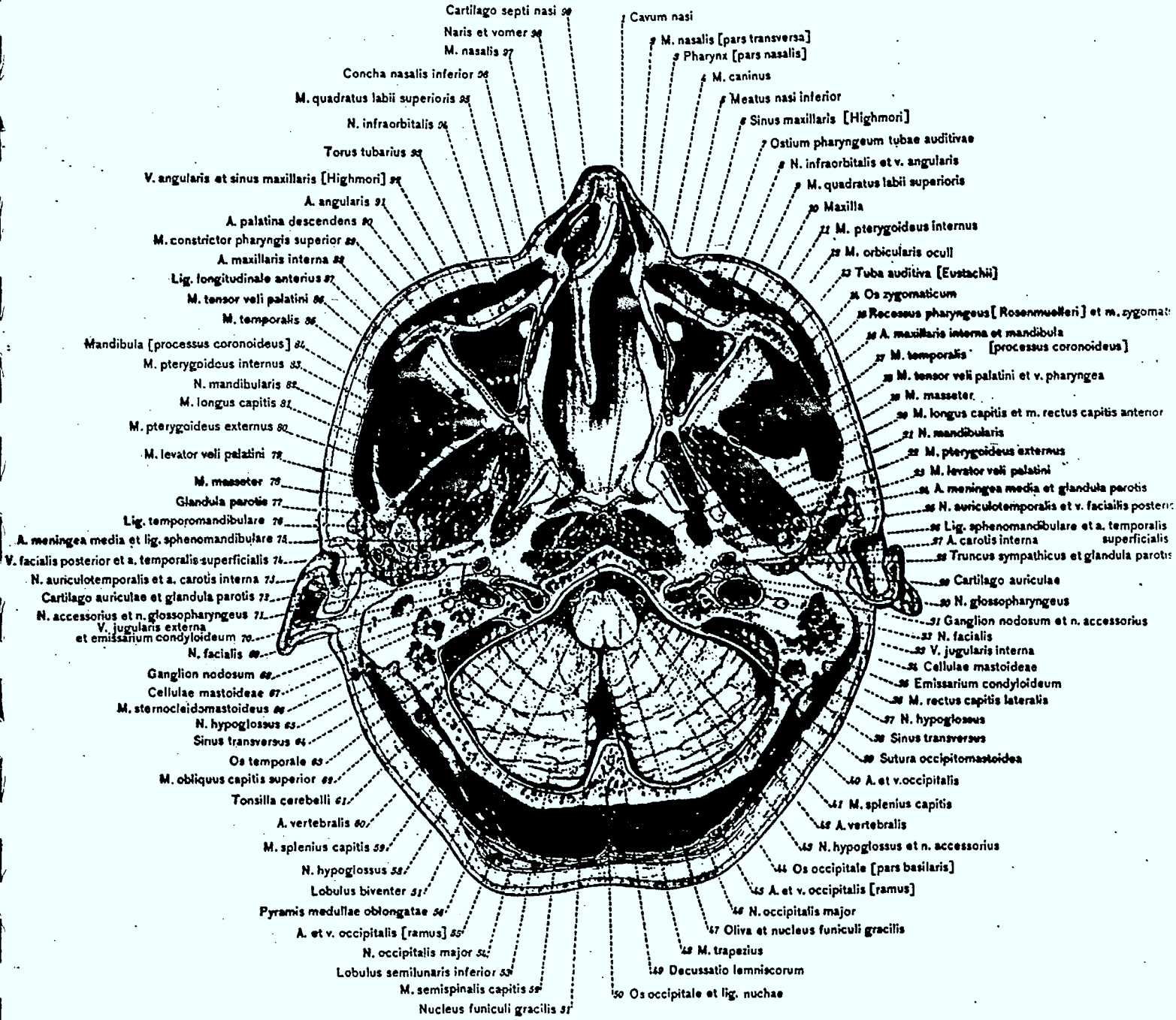
Cartilago septi nasi 96
Naris et vomer 96
M. nasalis 97
Concha nasalis inferior 96
M. quadratus labii superioris 95
N. infraorbitalis 94
Torus tubarius 93
V. angularis et sinus maxillaris [Highmori] 92
A. angularis 91
A. palatina descendens 90
M. constrictor pharyngis superior 89
A. maxillaris interna 88
Lig. longitudinale anterius 87
M. tensor veli palatini 86
M. temporalis 85
Mandibula [processus coronoideus] 84
M. pterygoideus internus 83
N. mandibularis 82
M. longus capitis 81
M. pterygoideus externus 80
M. levator veli palatini 79
M. masseter 78
Glandula parotis 77
Lig. temporomandibulare 76
A. meningea media et lig. sphenomandibulare 75
V. facialis posterior et a. temporalis superficialis 74
N. auriculotemporalis et a. carotis interna 73
Cartilago auriculae et glandula parotis 72
N. accessorius et n. glossopharyngeus 71
V. jugularis externa et emissarium condyloideum 70
N. facialis 69
Ganglion nodosum 68
Cellulae mastoideae 67
M. sternocleidomastoideus 66
N. hypoglossus 65
Sinus transversus 64
Os temporale 63
M. obliquus capitis superior 62
Tonsilla cerebelli 61
A. vertebralis 60
M. splenius capitis 59
N. hypoglossus 58
Lobulus biventer 57
Pyramis medullae oblongatae 56
A. et v. occipitalis [ramus] 55
N. occipitalis major 54
Lobulus semilunaris inferior 53
M. semispinalis capitis 52
Nucleus funiculi gracilis 51
Cavum nasi 1
M. nasalis [pars transversa] 2
Pharynx [pars nasalis] 3
M. caninus 4
Meatus nasi inferior 5
Sinus maxillaris [Highmori] 6
Ostium pharyngeum tubae auditivae 7
N. infraorbitalis et v. angularis 8
M. quadratus labii superioris 9
Maxilla 10
M. pterygoideus internus 11
M. orbicularis oculi 12
Tuba auditiva [Eustachii] 13
Os zygomaticum 14
Recessus pharyngeus [Rosenmuelleri] et m. zygomat
A. maxillaris interna et mandibula [processus coronoideus]
M. temporalis 17
M. tensor veli palatini et v. pharyngea 18
M. masseter 19
M. longus capitis et m. rectus capitis anterior 20
N. mandibularis 21
M. pterygoideus externus 22
M. levator veli palatini 23
A. meningea media et glandula parotis 24
N. auriculotemporalis et v. facialis posteri
Lig. sphenomandibulare et a. temporalis superficialis 26
A. carotis interna 27
Truncus sympathicus et glandula parotis 28
Cartilago auriculae 29
N. glossopharyngeus 30
Ganglion nodosum et n. accessorius 31
N. facialis 32
V. jugularis interna 33
Cellulae mastoideae 34
Emissarium condyloideum 35
M. rectus capitis lateralis 36
N. hypoglossus 37
Sinus transversus 38
Sutura occipitomastoidea 39
A. et v. occipitalis 40
M. splenius capitis 41
A. vertebralis 42
N. hypoglossus et n. accessorius 43
Os occipitale [pars basilaris] 44
A. et v. occipitalis [ramus] 45
N. occipitalis major 46
Oliva et nucleus funiculi gracilis 47
M. trapezius 48
Decussatio lemniscorum 49
Os occipitale et lig. nuchae 50

SECTION II

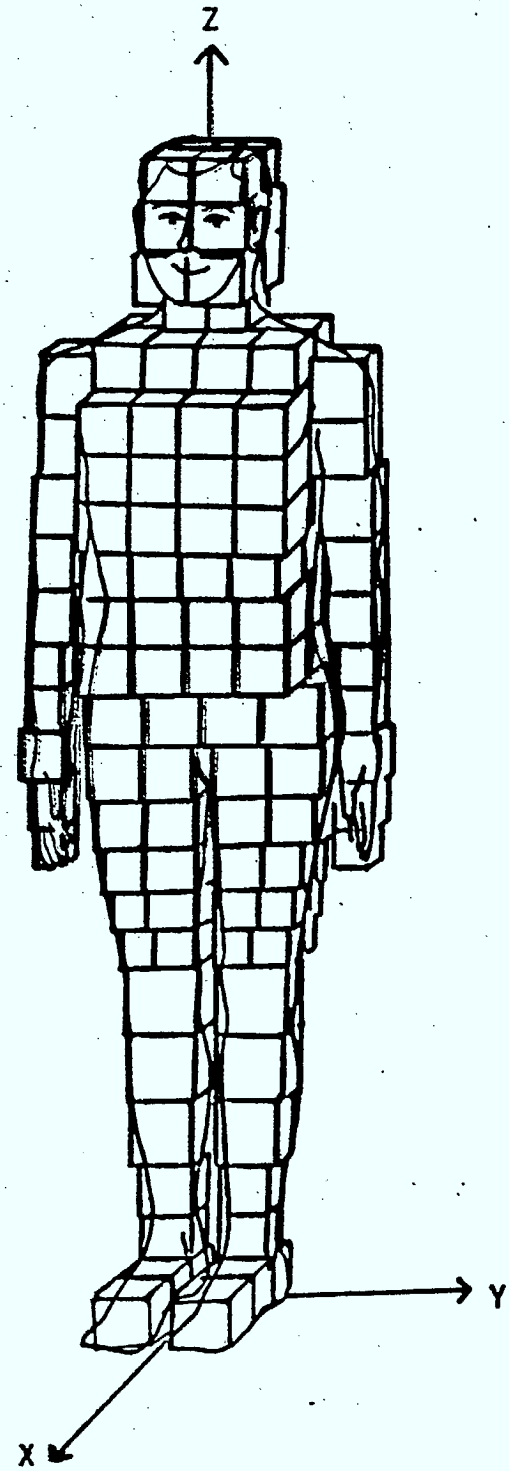

Figure 8-8 A 180-cell block human model of man. (From Hagmann et al. [1979]. *IEEE Trans. Microwave Theory Tech. 27*:804–809. © 1979 IEEE.)

from Gandhi, Om P., Ed., "Biological Effects and Medical Applications of Electromagnetic Energy," Prentice Hall, 1990, ISBN 0-13-082728-2.

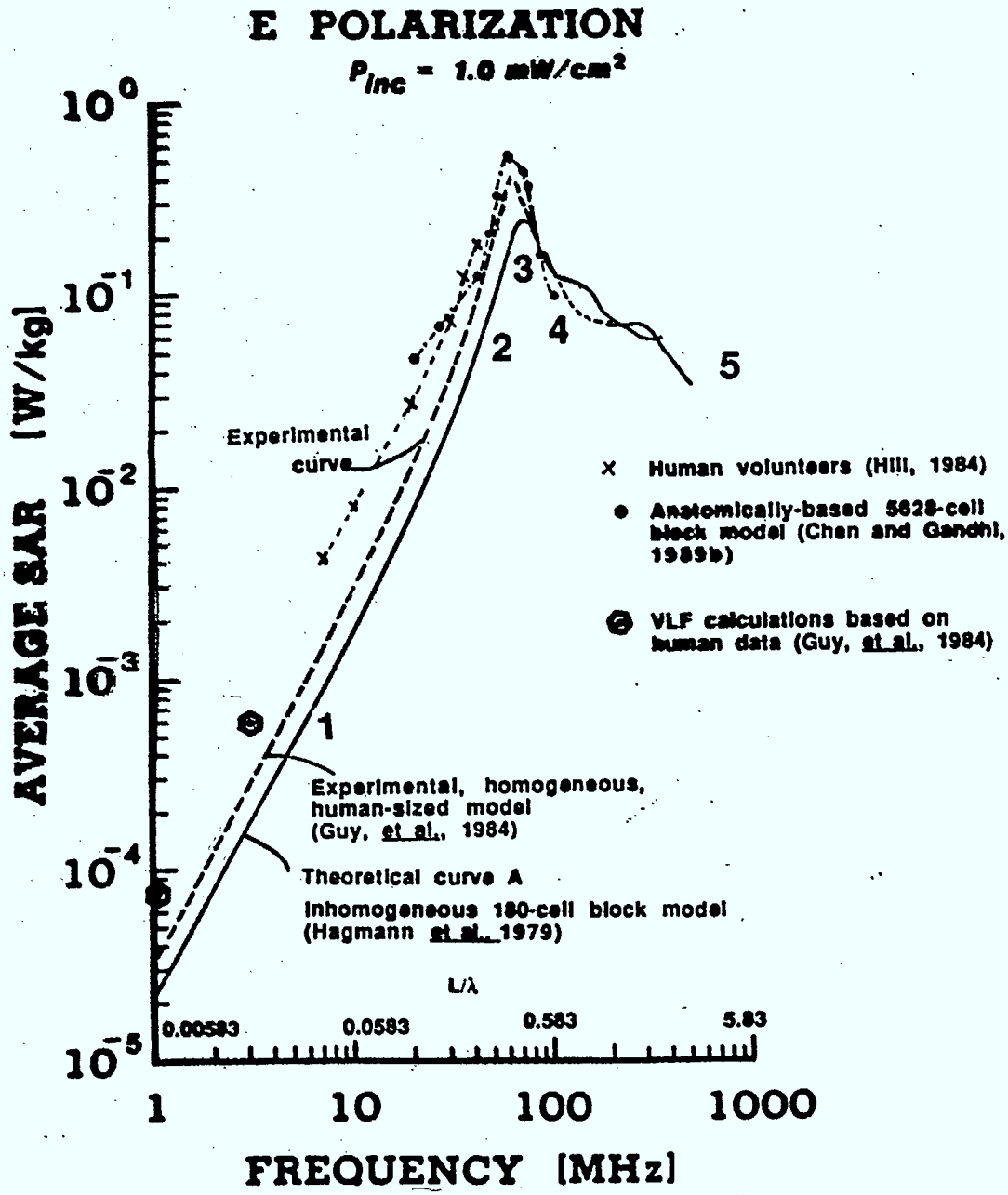

Figure 8-2 Comparison of theoretical and experimentally measured whole-body-averaged specific absorption rates for isolated man exposed at various frequencies.

from Gandhi, Om P., Ed., "Biological Effects and Medical Applications of Electromagnetic Energy," Prentice Hall, 1990, ISBN 0-13-082728-2.

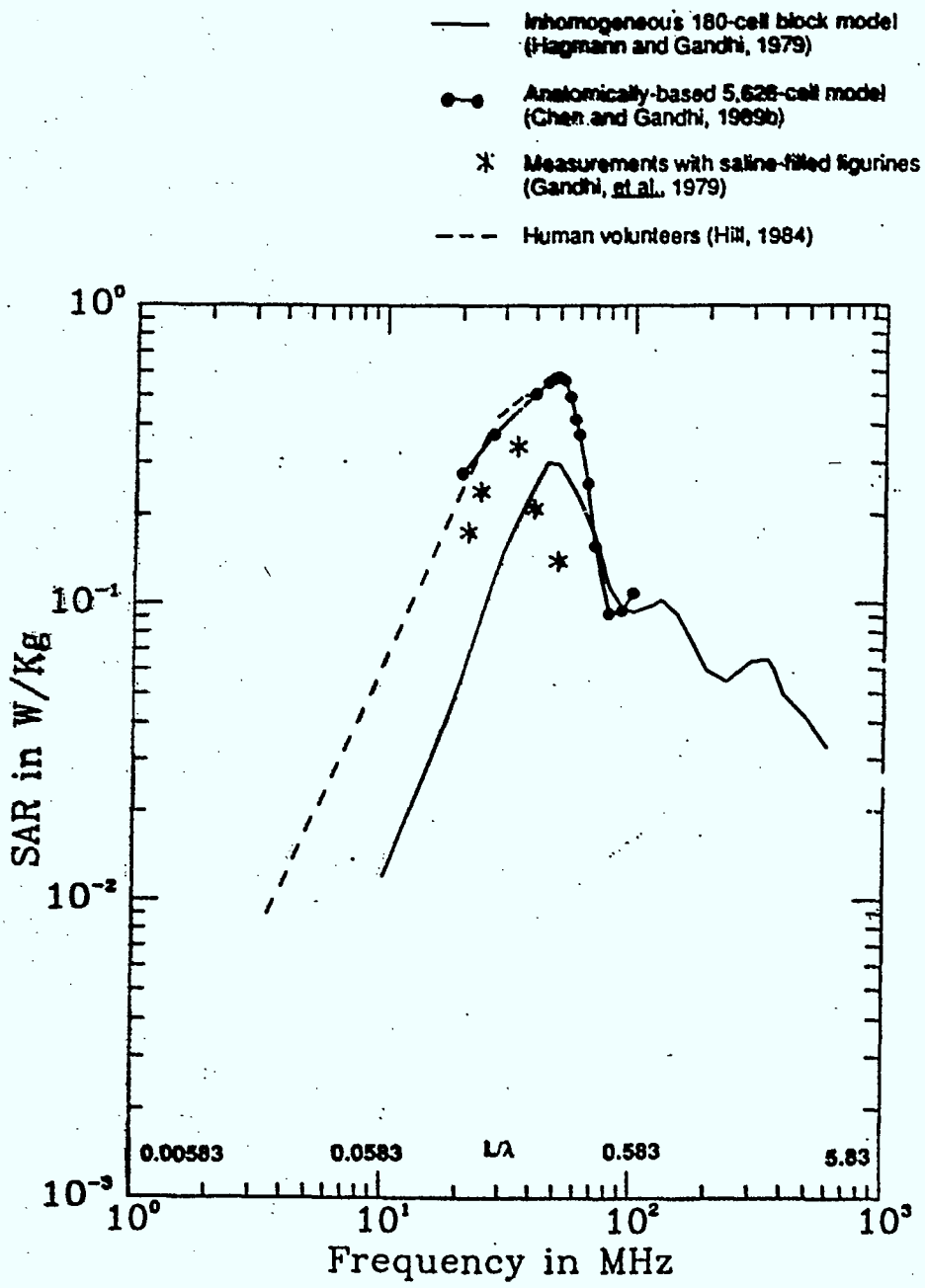

Figure 8-4 Comparison of theoretical and experimental whole-body-averaged specific absorption rates for grounded man exposed at various frequencies.

from Gandhi, Om P., Ed., "Biological Effects and Medical Applications of Electromagnetic Energy," Prentice Hall, 1990, ISBN 0-13-082728-2.

TABLE 1. (A) Composition by Weight of Muscle and Brain Equivalent Material. (B) Percentage by Volume of Filler Used in Lung Material. (C) Castable Bone Material Components. (D) Liquid Bone Material Components.

A. Muscle and brain material

Material	Percentage by weight	
	Muscle	Brain
Water	52.4	40.4
Salt (NaCl)	1.4	2.5
Sugar	45.0	56.0
HEC	1.0	1.0
Bacteriacide	0.1	0.1

B. Lung material

Material	Percentage by volume
Muscle material (above)	47
Microspheres	53

C. Bone material (castable)

Material	Percentage by weight
Two ton epoxy	
Epoxy	35.0
Hardener	35.0
KCl Solution	28.0

D. Bone material (liquid)

Material	Percentage by weight
TWEEN	57.0
n-Amyl alcohol	28.5
Paraffin oil	9.5
Water	4.5
Salt (NaCl)	0.5

from Hartsgrove, G., Kraszewski, A., and Surowiec, A., "Simulated Biological Materials for Electromagnetic Radiation Absorption Studies," Bioelectromagnetics 8:29-36 (1987), © Alan R. Liss, Inc.

TABLE 2. Dielectric Constant and Conductivity of Tissue Equivalent Materials at Selected Frequencies

	Frequency (MHz)					
	100		400		900	
Material	ϵ'	σ	ϵ'	σ	ϵ'	σ
Muscle	70.5	6.8	62.5	9.0	54.7	13.8
Brain	63.0	4.7	50.3	7.5	41.2	12.2
Lung	37.0	3.4	32.6	4.3	28.0	6.6
Bone cast	13.6	0.08	9.3	1.1	7.4	1.6
Bone liquid	10.8	0.35	9.1	0.66	7.2	1.2

from Hartsgrove, G., Kraszewski, A., and Surowiec, A., "Simulated Biological Materials for Electromagnetic Radiation Absorption Studies," Bioelectromagnetics 8:29-36 (1987), © Alan R. Liss, Inc.

PROPERTIES OF BIOMATERIALS

- Categorization
- Typical Values
- Dispersion Modelling - Hurt
- Recent Results - Furse, Chen, Ghandi, May 94

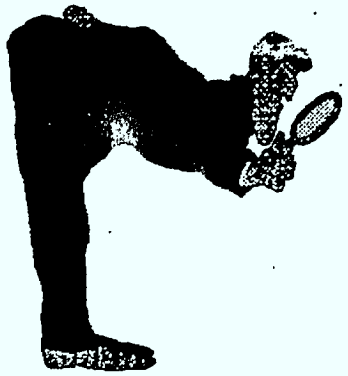

TABLE 5-3 Dielectric Constant at 37° C of Various Tissues at Radio and Microwave Frequencies

Tissue	Frequency					
	100 kHz	1 MHz	10 MHz	100 MHz	1 GHz	10 GHz
Skeletal muscle	$(14.4–24.8) \times 10^3$	$(1.9–2.5) \times 10^3$	162–204	64–90	57–59	43–45
Liver	$(9.8–13.7) \times 10^3$	1.97×10^3	251–338	65–82	47–49	35
Spleen	3.3×10^3	1.45×10^3	321–410	69–101	50–55	41
Kidney	$(10.9–12.5) \times 10^3$	$(2.39–2.69) \times 10^3$	190–204	66–95	42–50	40
Brain	$(1.96–3.8) \times 10^3$	$(0.54–1.25) \times 10^3$	163–352	57–90	37–55	38–44
Bone	280	87	37	23		

TABLE 5-4 Conductivity at 37° C of Various Tissues at Radio and Microwave Frequencies in Siemens per Meter

Tissue	Frequency					
	100 kHz	1 MHz	10 MHz	100 MHz	1 GHz	10 GHz
Skeletal muscle	0.38–0.59	0.58–0.85	0.69–0.96	0.75–1.05	1.38–1.45	11.5
Liver	0.15–0.16	0.27–0.3	0.42–0.47	0.6–0.72	0.95–1.1	8.9
Spleen	0.62	0.63	0.5–0.84	0.73–1.05	1.09–11.3	10.1
Kidney	0.24–0.25	0.36–0.37	0.50–0.68	0.66–1.05	0.95–1.0	9.7
Brain	0.12–0.17	0.14–0.21	0.21–0.63	0.48–0.95	0.81–1.2	8–10.8
Bone	0.014	0.017	0.024	0.057		

from Gandhi, Om P., Ed., "Biological Effects and Medical Applications of Electromagnetic Energy," Prentice Hall, 1990, ISBN 0-13-082728-2.

The Permittivity of Biological Materials at Various Frequencies

Tissue	Frequency (MHz) 10	27.12	100	350	400	500	750	900	1000	1500
Brain,	163-352		57-90						37-55	
nerve		155	52	60						
							49			46
			63		50.3			41.2		
				74						
Bone,	37		23							
Fat		29	7.5	5.7						
							5.6			5.6
			12.2		9.2			7.3		
				5.7						
Muscle	162-204		64-90						57-59	
		106	74	53						
							52			49
			70.5		62.5			54.7		
			71-76			52-54			49-52	
			63		52.6	52.4		52		
								50.5		
				54						
Skin		106	25	17.6						
							52			49
			57			46.5			43-46	
					17.4					
Eye		155	85	80						
							80			80
Blood		102	74	65						
			69-81			67-70			60.5	
				65						

6(c)

The Conductivity of Biological Materials at Various Frequencies

Tissue	Frequency (MHz) 10	27.12	100	350	400	500	750	900	1000	1500
Brain,	0.21-0.63		0.48-0.95						0.81-1.2	
nerve		0.45	0.53	0.65						
							1.2			1.4
			4.7		7.5			12.2		
				0.62						
Bone,	0.024		0.057							
Fat		0.04	0.07	0.072						
							0.09			0.12
			0.215		0.88			1.4		
				0.07						
Muscle	0.69-0.96		0.75-1.05						1.38-1.45	
		0.74	1.0	1.33						
							1.54			1.77
			6.8		9			13.8		
			0.62		0.68	0.72		0.92		
								1.2		
				1.3						
Skin		0.74	0.55	0.44						
							1.54			1.77
				0.42						
Eye		0.45	1.9	1.9						
							1.9			1.9
Blood		0.28	1.1	1.2						
				1.22						

DISPERSION

DEBYE EQUATION WITH 2 RELAXATION CONSTANTS

$$\epsilon^*(\omega) = \epsilon_0 \left[\epsilon_\infty + \frac{\epsilon_{s1} - \epsilon_\infty}{1 + j\omega\tau_1} + \frac{\epsilon_{s2} - \epsilon_\infty}{1 + j\omega\tau_2} \right] \quad \text{------} (4)$$

FURSE et al.

TABLE I

DEBYE CONSTANTS FOR TISSUES $\tau_1 = 46.25$ ns, $\tau_2 = 0.0907$ ns

(Average of optimum for fat and muscle.)

Tissue	ε_∞	ε_{s1}	ε_{s2}
Muscle	40.0	3948.	59.09
Bone / Cartilage	3.4	312.8	7.11
Blood	35.0	3563.	66.43
Intestine	39.0	4724.	66.09
Liver	36.3	2864.	57.12
Kidney	35.0	3332.	67.21
Pancreas / Spleen	10.0	3793.	73.91
1/3 Lung	10.0	1224.	13.06
Heart	38.5	4309.	54.58
Brain/Nerve	32.5	2064.	56.86
Skin	23.0	3399.	55.59
Eye	40.0	2191.	56.99

from Furse, Cynthia M., Chen, Jin-Yuan, and Gandhi, Om P., "The Use of the Frequency-Dependent Finite-Difference Time-Domain Method for Induced Current and SAR Calculations for a Heterogeneous Model of the Human Body," IEEE Transactions on EMC, Vol. 36, No. 2, May 1994, pp. 128-133.

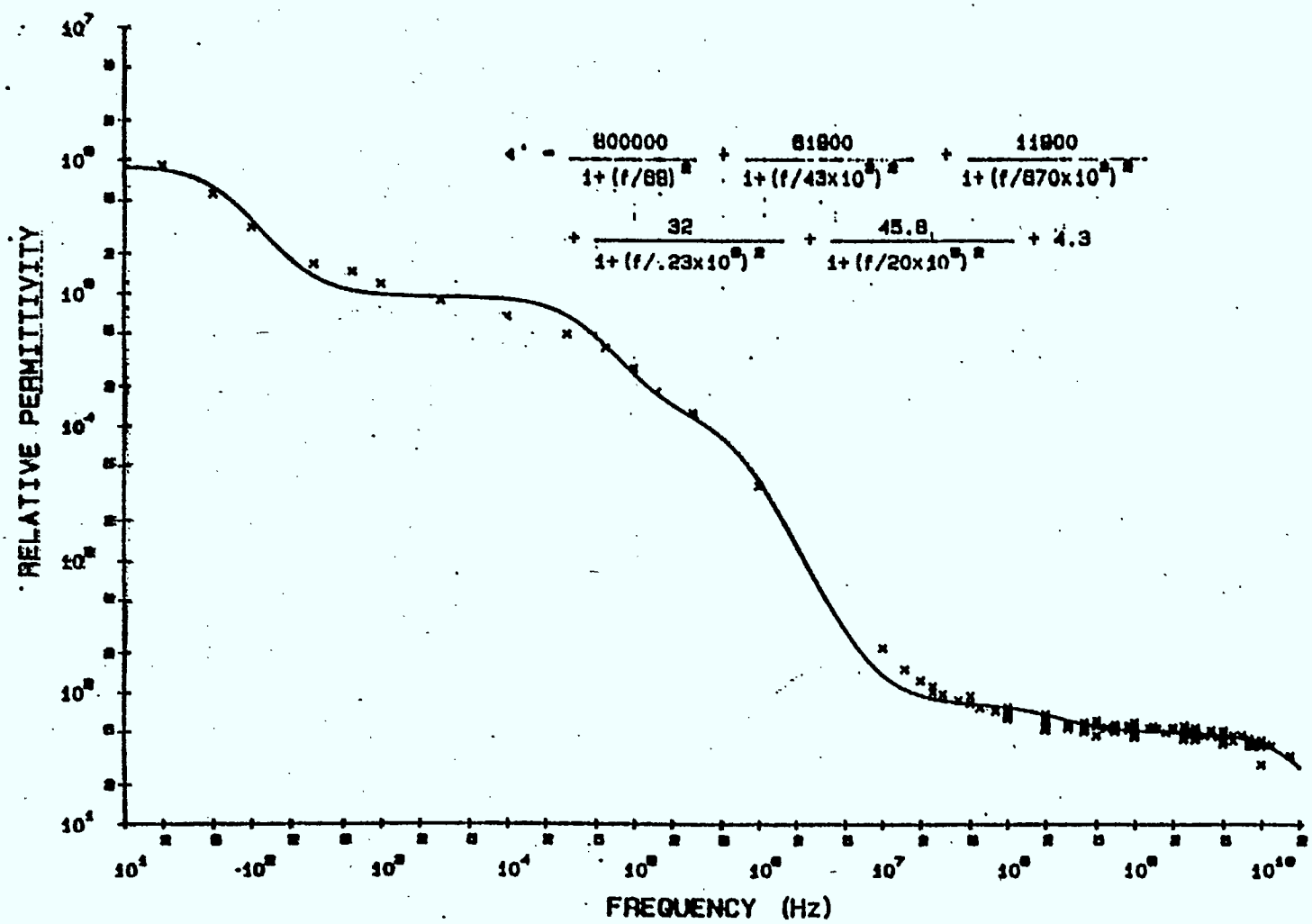

$$\epsilon' = \frac{800000}{1+(f/88)^2} + \frac{61800}{1+(f/43\times10^3)^2} + \frac{11900}{1+(f/870\times10^4)^2} + \frac{32}{1+(f/.23\times10^8)^2} + \frac{45.8}{1+(f/20\times10^8)^2} + 4.3$$

Fig. 1. Relative dielectric permittivity versus frequency: curve is best fit for five-term Debye expression to data (x's) found in Table I.

from Hurt, William D., "Multiterm Debye Dispersion Relations for Permittivity of Muscle," IEEE Transactions on Biomedical Engineering, Vol. BME-32, No. 1, January 1985, pp. 60-64.

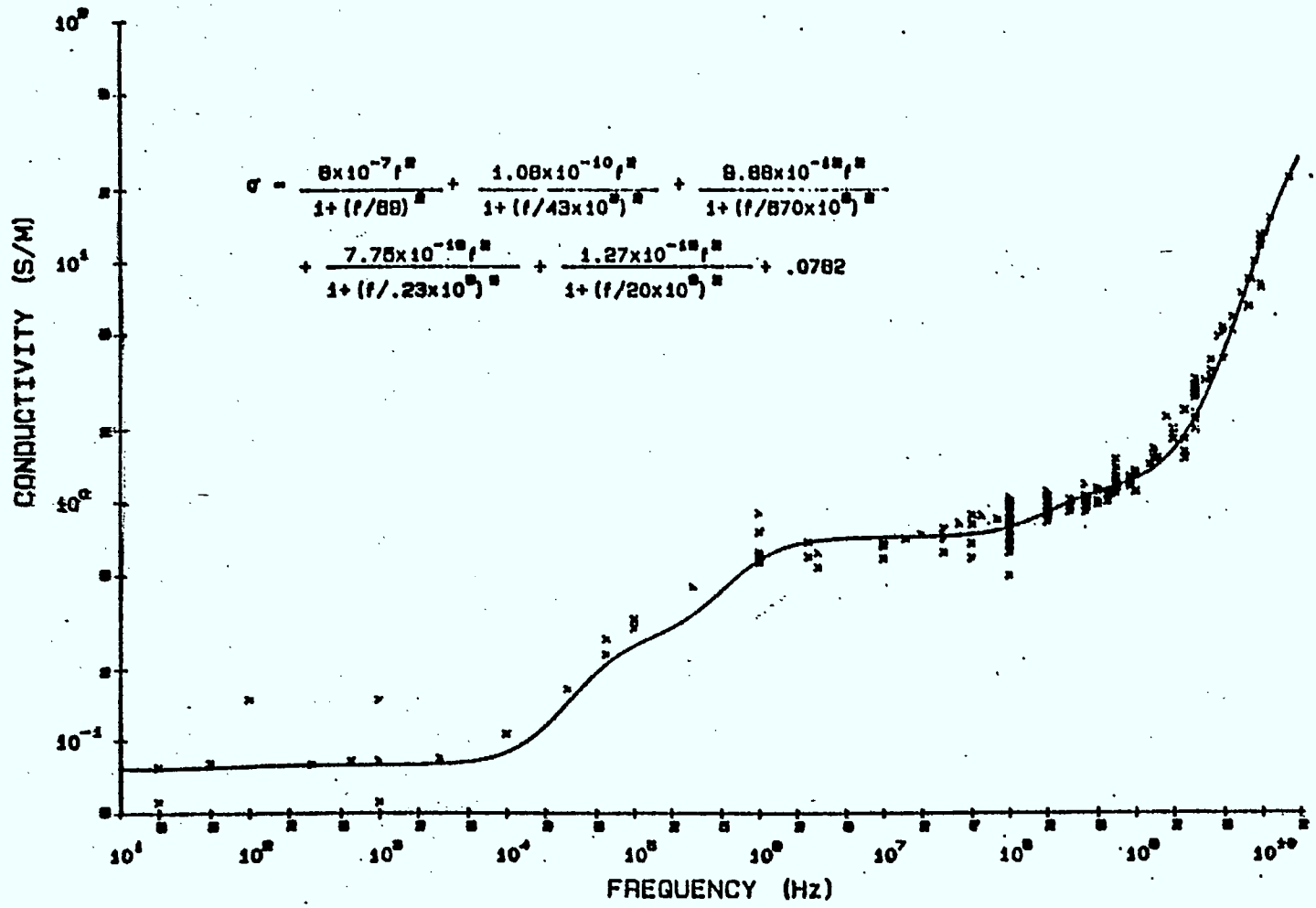

Fig. 2. Conductivity versus frequency: curve is best fit for five-term Debye expression to data (x's) found in Table I.

from Hurt, William D., "Multiterm Debye Dispersion Relations for Permittivity of Muscle," IEEE Transactions on Biomedical Engineering, Vol. BME-32, No. 1, January 1985, pp. 60-64.

•MEASUREMENTS & MODELLING

- Toftgard, Hornsleth, Bach Anderson, June 93
- Furse et al..., May 94
- DFL Measurements
- Deslile et al...
- Other

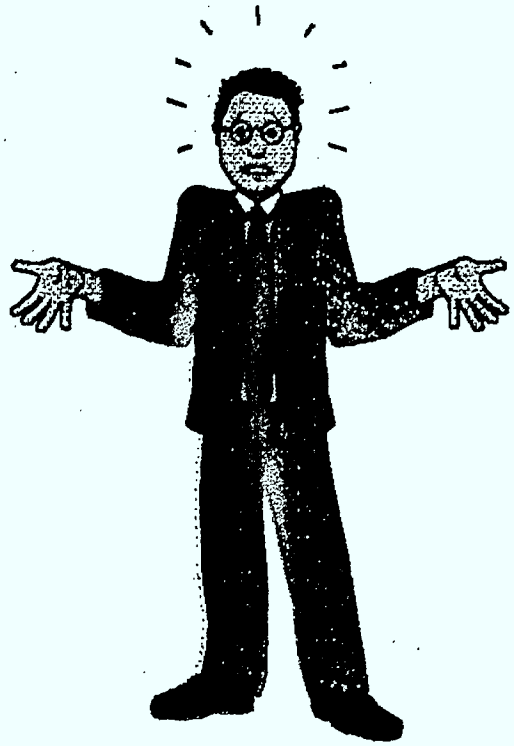

Antem 94

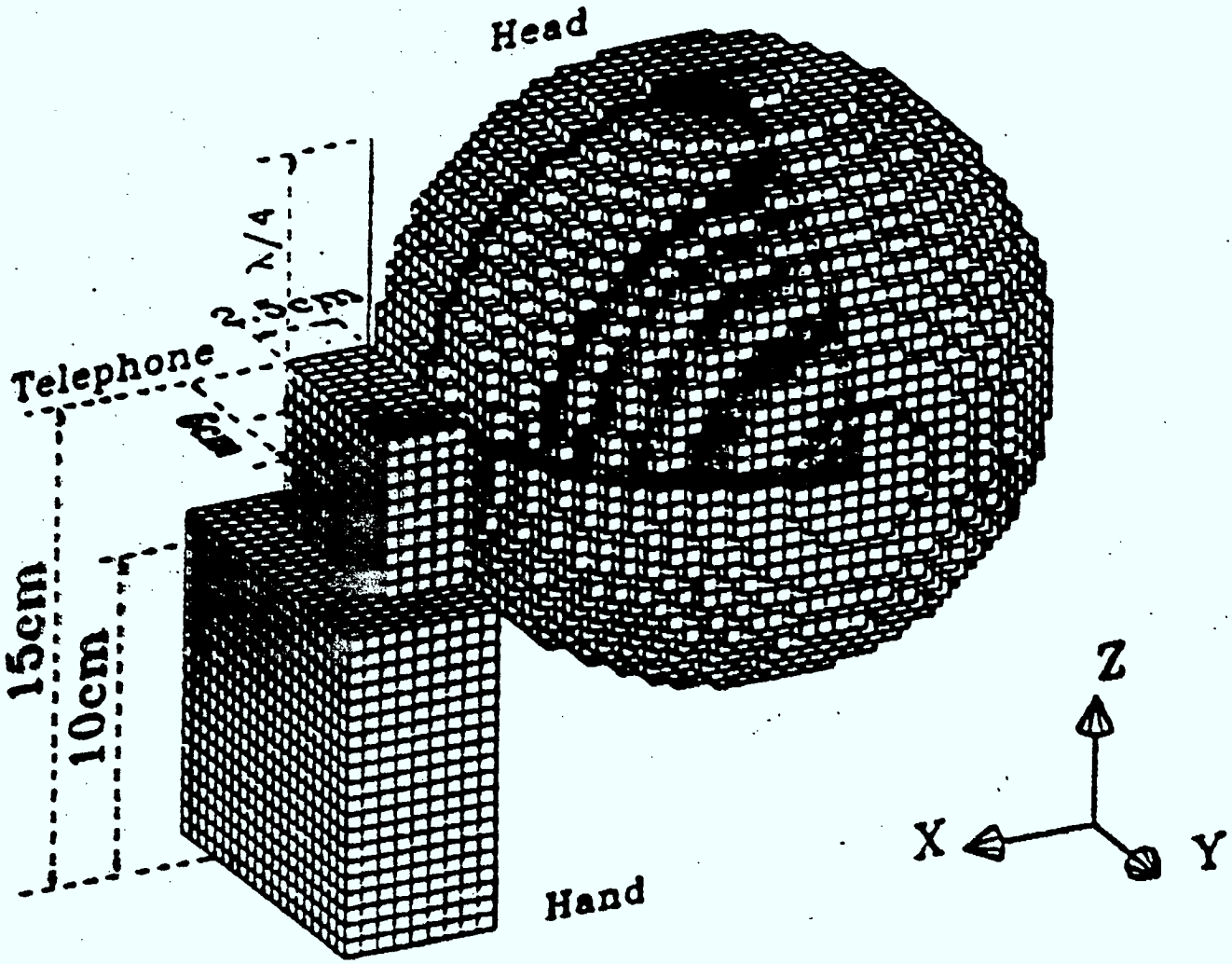

Fig. 1. The telephone-operator model used for the simulations. Both hand and head are modeled as pure muscle.

from Toftgård, Jørn, Hornsleth, Sten N., and Andersen, Jørgen Bach, "Effects on Portable Antennas of the Presence of a Person," IEEE Transactions on Antennas and Propagation, Vol. 41, No. 6, June 1993, pp. 739-746.

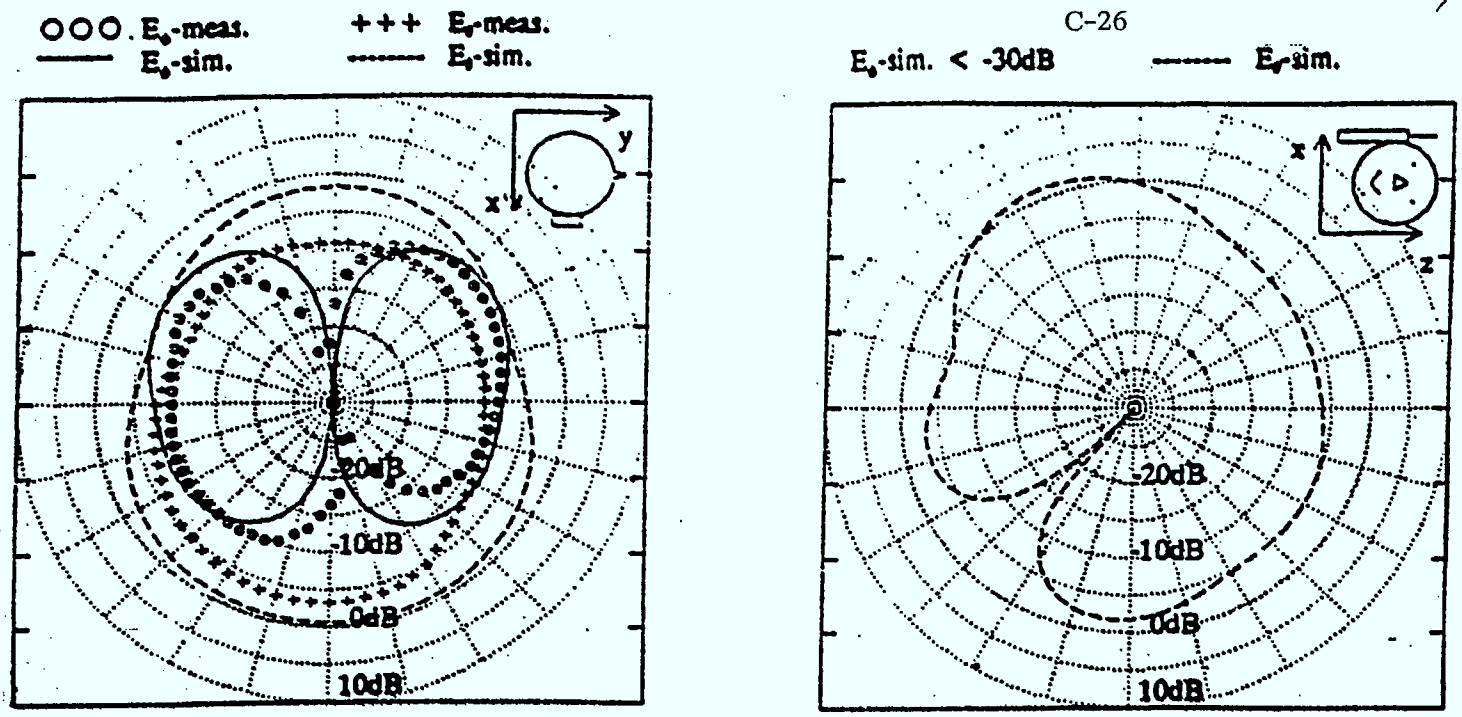

(a) (b)

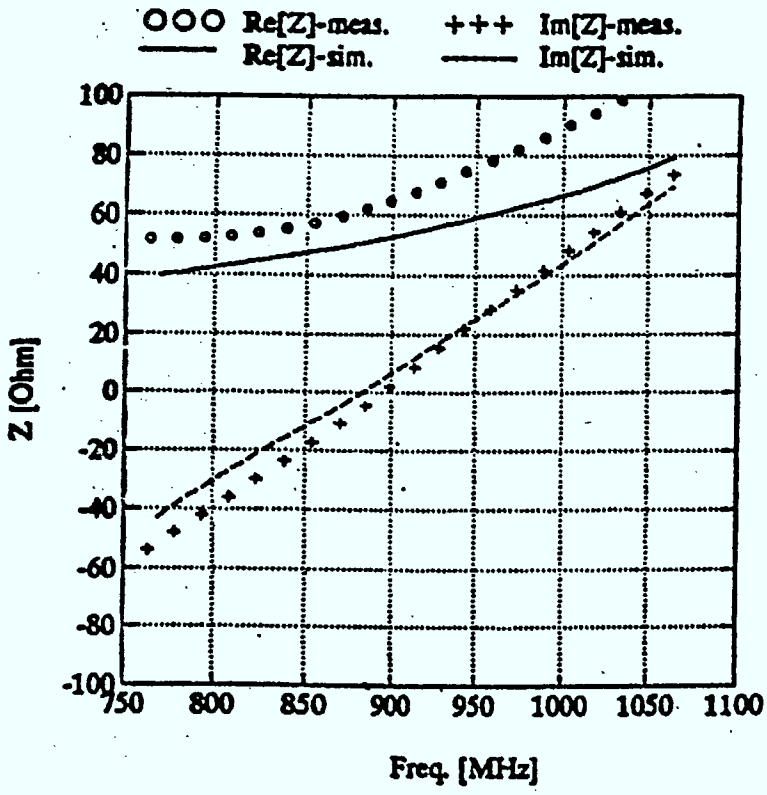

(c)

Fig. 3. Simulated and measured results for a $\lambda/4$ monopole mounted on the telephone with the operator included for $f = 914$ MHz. (a) Radiation pattern in the XY plane. (b) Radiation pattern in the XZ plane. (c) Input impedance.

from Toftgård, Jørn, Hornsleth, Sten N., and Andersen, Jørgen Bach, "Effects on Portable Antennas of the Presence of a Person," IEEE Transactions on Antennas and Propagation, Vol. 41, No. 6, June 1993, pp. 739-746.

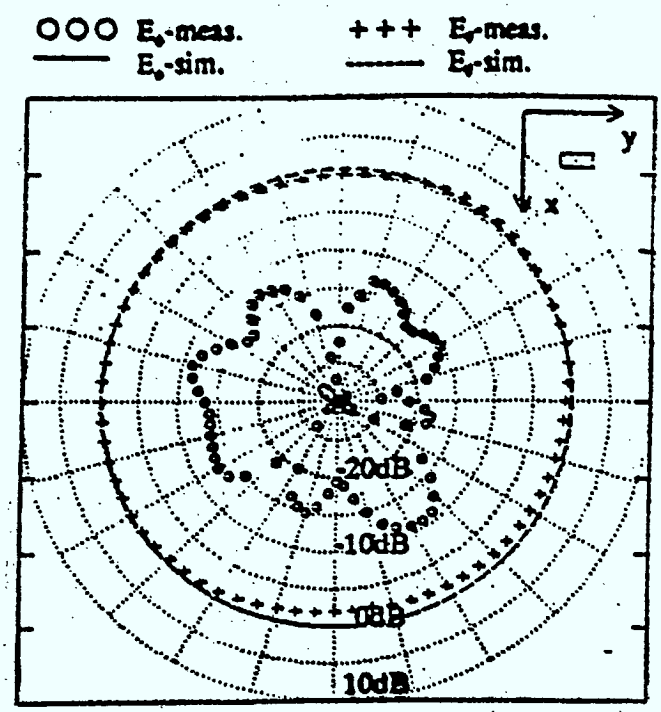

(a)

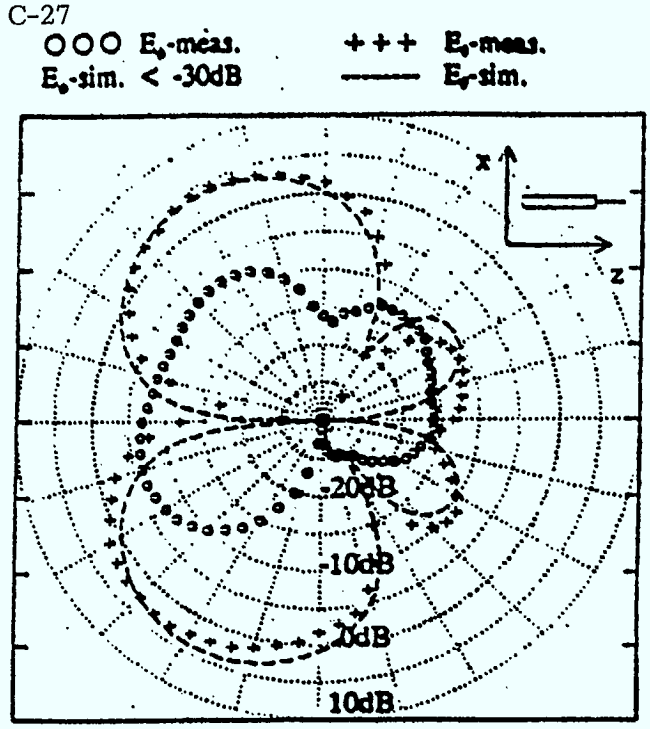

(b)

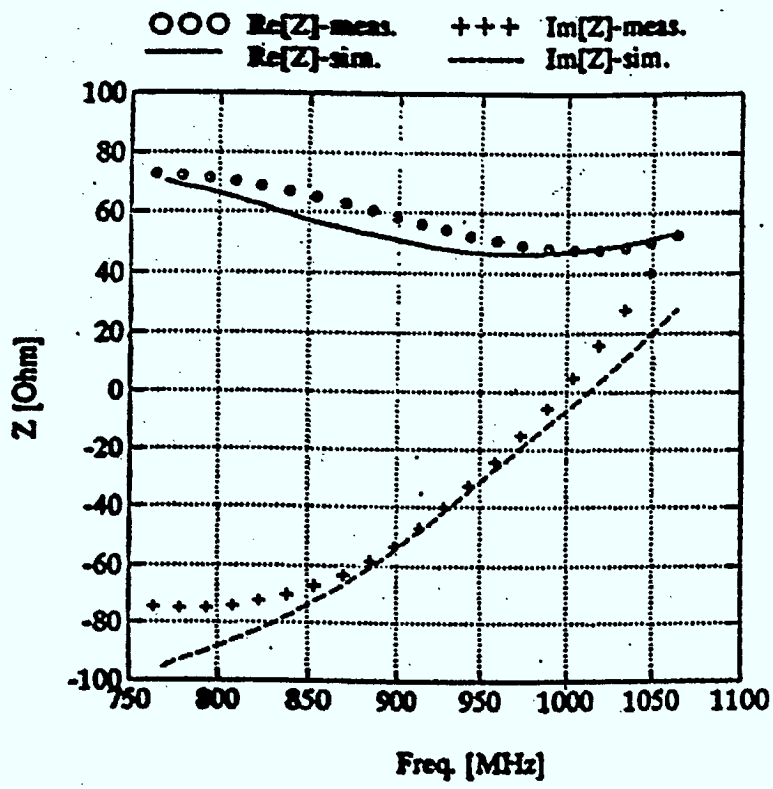

(c)

Fig. 2. Simulated and measured results for a $\lambda/4$ monopole mounted on the telephone without the operator included for f = 914 MHz. (a) Radiation pattern in the XY plane. (b) Radiation pattern in the XZ plane. (c) Input impedance.

from Toftgård, Jørn, Hornsleth, Sten N., and Andersen, Jørgen Bach, "Effects on Portable Antennas of the Presence of a Person," IEEE Transactions on Antennas and Propagation, Vol. 41, No. 6, June 1993, pp. 739-746.

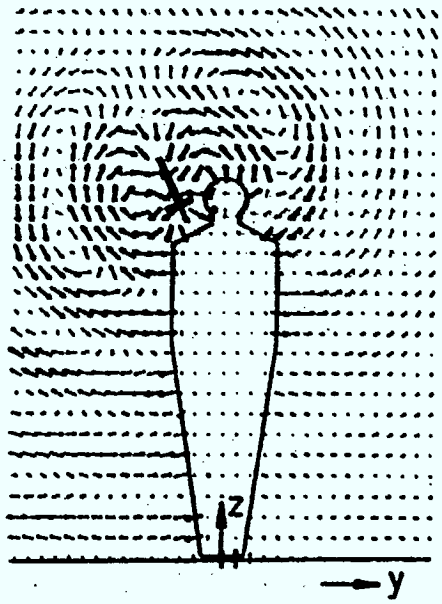

a) Near field distribution ($\omega t=0$)

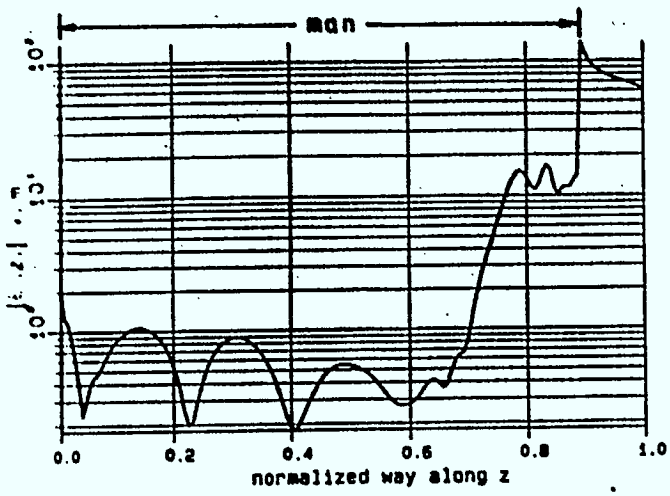

b) Field strength along the z axis

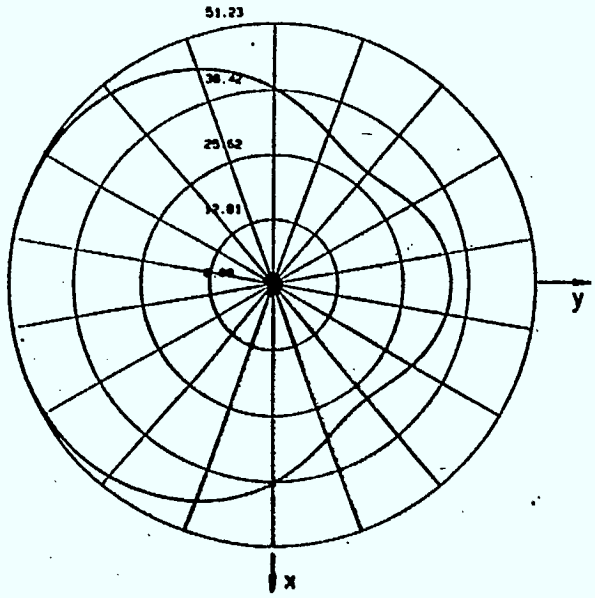

c) Far field horizontal diagram (maximum value corresponds to 51.2 mV/m at a distance of 1000 m)

Fig. 6: Electric field of a hand-held transmitter with inclined antenna (27.5°) at 430 MHz

from Brüns, H.-D., Singer, H., and Mader, T., "Field Distributions of a Hand-Held Transmitter Due to the Influence of the Human Body," 10th International Zurich Symposium and Technical Exhibition on EMC, March 9-11, 1993, Session on Biological Effects, pp. (3A3) 9-14.

FDTD MODEL PARAMETERS

- Paper list:
- Cell Size (~ 3.1 mm)
- White Space ~ 30
- ABC - 2nd order
- Source - Luebbers --
- Dispersion - later
- Output

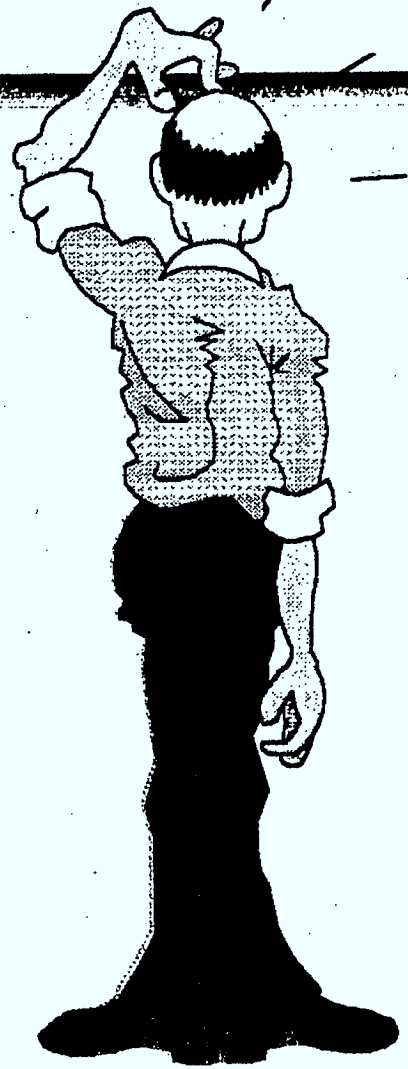

Antem 94

NEXT STEPS - CONCLUSION

- Search for Models, Codes & Data
- Codes - External Problem
- Model Development
  - FDTD Code Refinement
  - Concurrent Measurement Program/Validation
  - Contact with Community

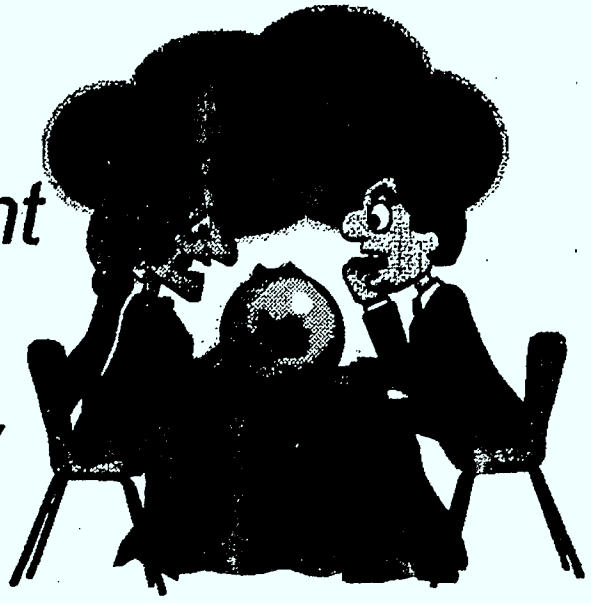

Antem 94

s11 a25.dat

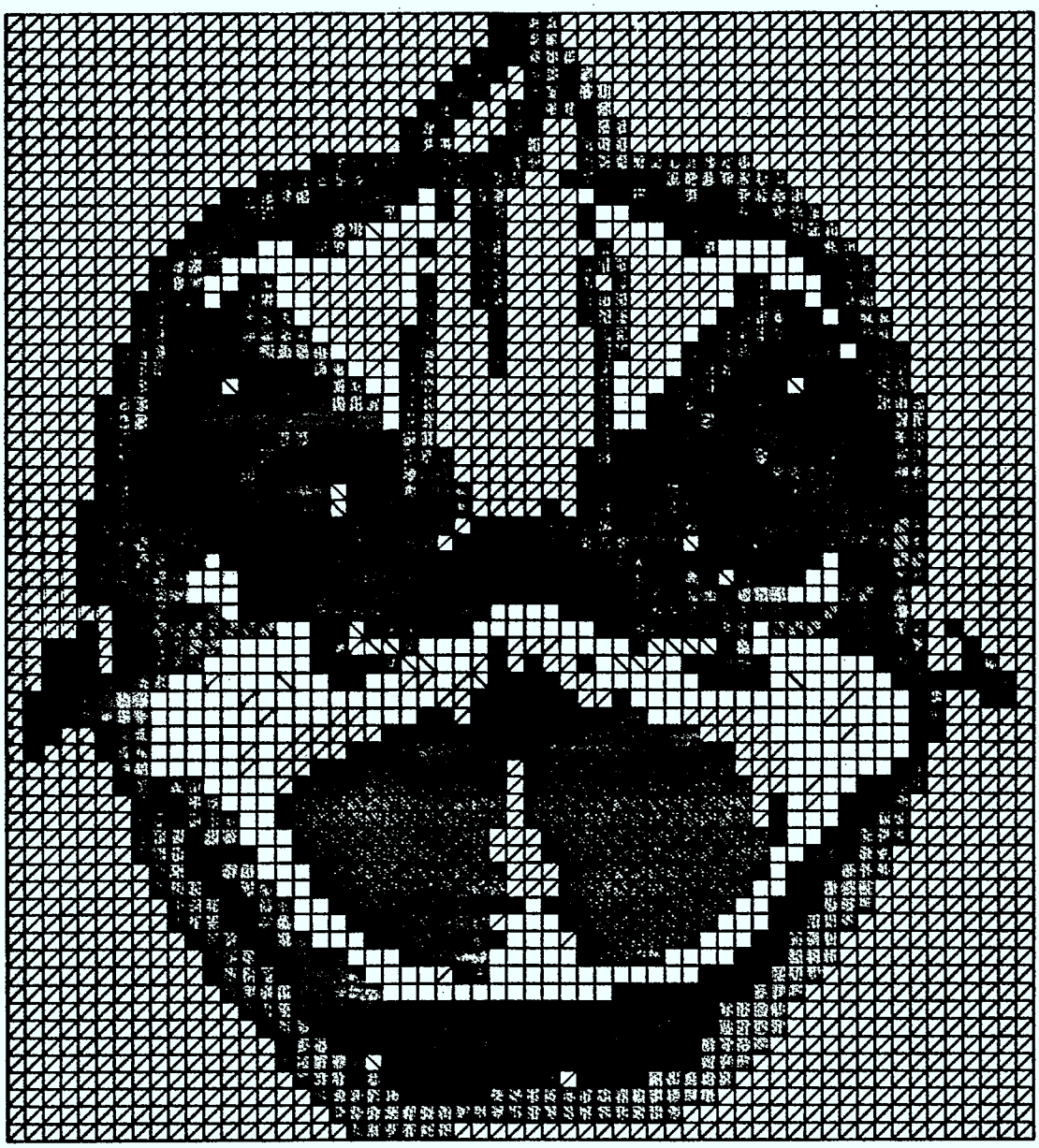

- FREE SPACE
- LIGAMENT
- HYPOPHYSE
- C INTERNAL
- GLA SUBMAX
- V QUARTUS
- TONS/GANG
- GLAND
- VERMIS
- CER PEDUNC
- PONS
- HIPPOCAMPI
- NERVE
- FORNIX
- PUTAMEN
- V TERTIUS
- M INT,C MA
- CARTILAGE
- NUCLEUS
- BLOOD
- C CALLOSUM
- GREY BR
- WHITE BR
- EYE
- SKIN
- V LATERAL
- BONE,FAT
- MUSCLE

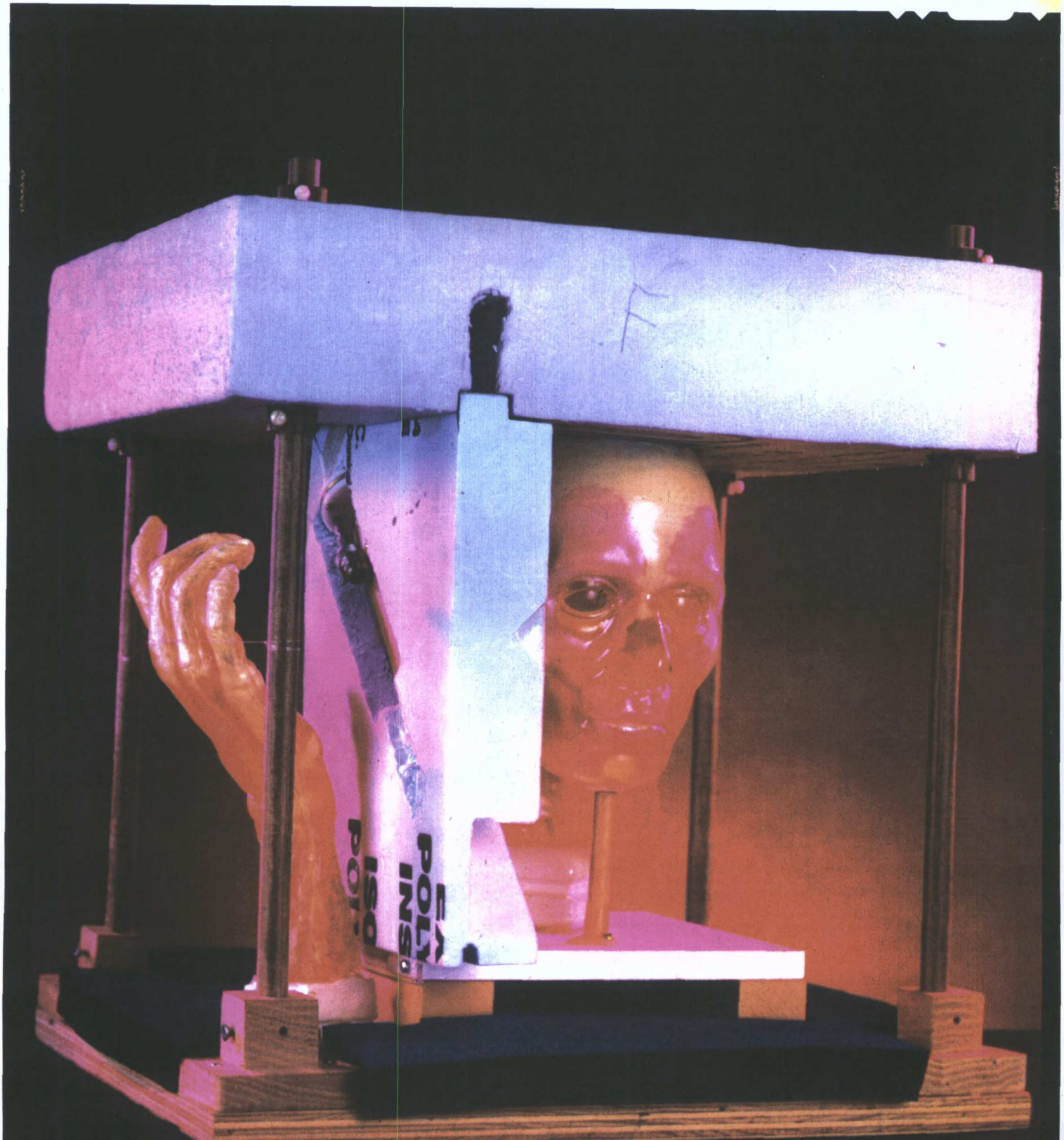
POLY
INSD
POL.